



Long-term air concentrations, wet deposition, and scavenging ratios of inorganic ions, HNO₃ and SO₂ and assessment of aerosol and precipitation acidity at Canadian rural locations

Irene Cheng and Leiming Zhang

5 Air Quality Research Division, Science and Technology Branch, Environment and Climate Change Canada, 4905 Dufferin Street, Toronto, Ontario, M3H 5T4, Canada

Correspondence to: Irene Cheng (irene.cheng@canada.ca)

Abstract. This study analyzed long-term air concentrations and annual wet deposition of inorganic ions and aerosol and precipitation acidity at 30 Canadian sites from 1983-2011. Scavenging ratios of inorganic ions and relative contributions of particulate- and gas-phase species to NH₄⁺, NO₃⁻, and SO₄²⁻ wet deposition were determined. Long-term median atmospheric NH₄⁺, NO₃⁻, and SO₄²⁻ between sites ranged from 0.1-1.7, 0.03-2.0, and 0.6-3.5 μg m⁻³, respectively. Their median annual wet deposition varied from 0.2-5.8, 0.8-23.3, and 0.8-26.6 kg ha⁻¹ a⁻¹. Geographical patterns of atmospheric Ca²⁺, Na⁺, Cl⁻, NH₄⁺, NO₃⁻, and SO₄²⁻ were similar to wet deposition and attributed to anthropogenic sources, sea-salt emissions, and agricultural emissions. Decreasing trends in atmospheric NH₄⁺ (1994-2010) and SO₄²⁻ (1983-2010) were prevalent. Atmospheric NO₃⁻ increased from 1991-2001 and declined from 2001-2010. These results are consistent with SO₂, NO_x and NH₃ emission trends in Canada and the U.S. Widespread declines in annual NO₃⁻ and SO₄²⁻ wet deposition ranged from 0.07-1.0 kg ha⁻¹ a⁻¹ (1984-2011). Acidic aerosols and precipitation impacted southern and eastern Canada more than western Canada; however both trends have been decreasing since 1994. Scavenging ratios of particulate NH₄⁺, SO₄²⁻ and NO₃⁻ differed from literature values by 22%, 44% and a factor of 6, respectively, because of the exclusion of gas scavenging. Average gas and particle scavenging contributions to wet NO₃⁻ deposition were 72±23% for HNO₃ and 28±23% for particulate NO₃⁻. SO₂ and particulate SO₄²⁻ contributed 37±20% and 63±20% to wet SO₄²⁻ deposition, respectively. NH₃ and particulate NH₄⁺ contributed 30±19% and 70±19% to wet NH₄⁺ deposition.



1 Introduction

The Canadian Air and Precipitation Monitoring Network (CAPMoN) measures trace gas concentrations and particulate inorganic ion concentrations in air and precipitation at rural locations across Canada. Since 1983, the network has been collecting filter and precipitation samples and the number of sites has expanded to 33 as of 2010. CAPMoN was developed to monitor trends in atmospheric pollutants contributing to smog and acid rain, and the data was later used to assess the impacts of environmental policies in the Canada-U.S. Air Quality Agreement. This bilateral agreement signed in 1991 recognizes the impacts of transboundary pollution and sets objectives to reduce SO₂ and NO_x emissions.

In this study, the focus is on the particulate base cations (Ca²⁺, Mg²⁺, K⁺, Na⁺, NH₄⁺) and acidic anions (Cl⁻, NO₃⁻, and SO₄²⁻), nitric acid, and sulfur dioxide that have direct impacts on acid rain. Nitrates and sulfates in acid rain reduce soil quality by causing the depletion of base cations, which are plant nutrients and are also involved in neutralizing acids. Base cations in soil can be replenished by mineral weathering, deposition, wind erosion, agricultural tilling, and forest fires (Hedin et al., 1994; Driscoll et al., 2001). However, when acidic deposition exceeds the supply of base cations, soil acidification occurs. Soil acidity has consequently increased the leaching of inorganic aluminum (Al) monomers, which is a toxic form of Al to plants and animals (Driscoll et al., 2001). Trees (e.g., red spruces and sugar maples) experienced damage to foliage, decreased adaptability to cold climates, slower growth, and mortality during 1960s-1980s from direct and indirect impacts of acid rain (Driscoll et al., 2001; Watmough and Dillon, 2003). Acid rain and runoff of acidic soil also increased nitrates, sulfates and inorganic Al and reduced pH in surface waters of Atlantic Canada, southcentral Ontario, and northeastern U.S. (Clair et al., 2002; Driscoll et al., 2003; Jeffries et al., 2003). Lake acidification has led to detrimental effects including mortality on zooplankton and fish (Driscoll et al., 2001 and references therein). Terrestrial birds are also impacted because when calcium is depleted from soil, less calcium-rich insects are available for birds to consume (Hames et al., 2002). Calcium deficiency in birds can cause eggshell thinning and other reproductive consequences (Hames et al., 2002).

Assessments of lake acidification in the previous decade indicate declines in nitrates and sulfates in surface water, some improvements to pH and acid neutralizing capacity, and conversion to less toxic organic Al (Clair et al., 2002; Driscoll et al., 2003; Jeffries et al., 2003; Kothawala et al., 2011; Strock et al., 2014). Although nitrate and sulfate deposition have been decreasing, surface water conditions have not improved at the same rate because nitrates and sulfates that have accumulated in soil and wetlands over a long period of time is gradually releasing to surface waters (Stoddard et al., 1999; Driscoll et al., 2001; Clair et al., 2002; Jeffries et al., 2003). A recent assessment by Lawrence et al. (2015) indicates no additional soil acidification and that acid deposition effects on soil have started to diminish in northeastern U.S. and eastern Canada according to indicators, such as exchangeable Ca and Al, base cations, and pH levels. Considering the role of inorganic ions on acid deposition effects on biota, it is important to continually study the wet deposition of inorganic ions.



The wet deposition of particulate base cations and acidic anions depend on the particulate concentrations of these inorganic ions in air and some trace gases, such as nitric acid and sulfur dioxide. This simplified relationship is the premise behind the scavenging ratio, defined as a ratio of a pollutant's concentration in precipitation to that in air. In reality, wet deposition is a very complex process that involves an understanding of cloud and precipitation processes and aqueous phase chemistry, which are considered to be the major sources of uncertainty in wet deposition modeling (Tost et al., 2007; Kajino and Aikawa, 2015). Scavenging ratios can be considered a measure of the wet scavenging efficiency of air pollutants, since they have been used to compare the precipitation removal of different pollutants in previous studies (Galloway et al., 1993; Guerzoni et al., 1995; Tuncel and Ungör, 1996; Shrestha et al., 2002; Hicks et al., 2005; Kulshrestha et al., 2009; Bourcier et al., 2012; Zhang et al., 2015). These studies demonstrated that scavenging ratios vary according to particle size distribution similar to the particle size dependency of scavenging coefficients typically used in wet deposition modeling (Wang et al., 2014). Thus, scavenging ratios of particulate-phase pollutants have been used as a surrogate for other particulate-phase pollutants with similar particle sizes (Cadle et al., 1990; Sakata and Asakura, 2007; Cheng et al., 2015).

The objectives of this study were to (1) analyze long-term geographical patterns and temporal trends in nitric acid and sulfur dioxide concentrations and the air concentrations and wet deposition of base cations and acidic anions; (2) examine geographical and temporal trends in aerosol acidity and acid rain; (3) determine scavenging ratios for particulate inorganic ions using precipitation and air concentrations; and (4) develop an approach for estimating particulate and gaseous species wet scavenging contributions to total nitrate, ammonium and sulfate wet deposition and their scavenging ratios.

2 Methodology

2.1 Data description

2.1.1 CAPMoN datasets

24-hr integrated trace gas concentrations and particulate inorganic ion concentrations in air and precipitation are measured by CAPMoN at rural locations across Canada. This dataset was accessed online from the NAtChem database (Environment Canada, 2015a). The monitoring sites are located in various regions of Canada with the majority of the sites residing in the province of Ontario and Quebec (Fig. S1). Site elevations range from 14-707 m.a.s.l. The sites include continental and coastal sites, and the land use types of most CAPMoN sites are categorized as forested or agricultural sites (Table 1). Only the sites with long-term data (≥ 9 years) were analyzed in this study. The measurement periods are not synchronized between all sites; therefore, some sites may have different starting and end dates.

2.1.2 Air concentrations



Non-size selective filters are used to collect air samples, which are analyzed for major inorganic ions (Ca^{2+} , Mg^{2+} , K^+ , Na^+ , Cl^- , NH_4^+ , NO_3^- , and SO_4^{2-}) and HNO_3 and SO_2 trace gases. Teflon filters are used for the inorganic ions, while nylon and impregnated cellulose filters are used for HNO_3 and SO_2 , respectively. The filters are placed in a three stage filter pack, which samples air at 10 m above ground. Every 24 hr at 8:00 LT, the sequential sampler passes air through a different filter pack. The filters are retrieved and delivered to CAPMoN laboratories for chemical analysis. The collected mass for each species, blank values, and mass flow rates are used to determine the air concentrations in $\mu\text{g m}^{-3}$. Quality control of the data are performed using the Research Data Management and Quality Assurance System (RDMQTM) software (McMillan et al., 2000), which processes and manages large amounts of data, applies quality control checks, and assigns validity flags to each data point. The standard data flags warn users of missing values, invalidated values, valid values below detection limit, valid estimated and interpolated values, non-conforming sampling periods, and valid values that have been replaced by the detection limit. In this study, valid air concentrations from 16 sites were analyzed. Available air measurements between 1983 and 2010 at the 16 sites are shown in Table 1.

2.1.3 Precipitation concentrations

Precipitation is sampled using a wet-only precipitation collector, which automatically opens when sensors detect precipitation. Precipitation is collected in a specially-designed plastic bag in the collector. The bags containing precipitation are retrieved each day between 8:00 and 9:00 LT and are sealed, weighed and then kept refrigerated. The 24-hr integrated precipitation samples are analyzed for H^+ and major inorganic ions (described in Sect. 2.1.2) in concentrations of mg l^{-1} . Precipitation amount is also recorded daily at the precipitation monitoring sites for the determination of wet deposition flux. Standard data flags similar to the air data are applied to the precipitation data. In this study, valid precipitation concentrations from 30 sites were analyzed. Available precipitation measurements between 1984 and 2011 at the 30 sites (two collocated collectors at Egbert) are shown in Table 1.

2.1.4 Meteorological data

Hourly air temperature, relative humidity and wind direction data at collocated or nearby stations to CAPMoN sites were obtained from the Canadian Climate Data Archives (Environment Canada, 2015b). Hourly air temperature and relative humidity were averaged to daily values to correspond with the sampling intervals of the air and precipitation concentrations. Hourly wind direction data were used to determine the prevailing wind directions at each site.

2.2. Data analysis

2.2.1 Long-term patterns

Geographical patterns and temporal trends in air concentrations and wet deposition were examined. The geographical patterns in air concentrations were based on 24-hr integrated measurements. For wet deposition, geographical patterns in the



annual wet deposition flux were analyzed since annual wet deposition is typically reported in previous studies. Daily precipitation concentrations were multiplied by the corresponding daily precipitation amount above the rain gauge detection limit of 0.2 mm. The annual wet deposition flux was obtained by summing the daily wet deposition flux. Thus, only the years with complete wet deposition data are used to determine the annual wet deposition. Statistical analyses of temporal trends were performed using regression analysis of the annual average air concentrations and annual wet deposition for all years with complete data. The Mann-Kendall Test and Seasonal Kendall Test were also applied to the annual wet deposition and annual average air concentrations, respectively, to assess whether there was a statistically significant monotonic trend (Gilbert, 1987; Prestbo and Gay, 2009; Zbieranowski and Aherne, 2011; Cole et al., 2014). The Seasonal Kendall and Sen's estimator of slope provides the magnitude of the temporal trend on a per year basis. The Seasonal Kendall test is similar to the Mann-Kendall test, except it analyzes the temporal trend in each month separately (Gilbert, 1987). The Mann-Kendall test was used to obtain the annual wet deposition trend because the magnitude of the slope (trend) based on monthly total wet deposition (if the Seasonal Kendall test was applied) is inconsistent with that of the annual wet deposition trend since wet deposition depends on the precipitation amount. The relationship between meteorological factors and temporal trends in air concentrations and wet deposition were also examined by correlation analysis.

2.2.2 Aerosol acidity

The molar cation/anion charge equivalent ratio (c/a) (Hennigan et al., 2015) was used as a measure of H^+ and aerosol acidity for the air sampling sites. The ions associated with acidic aerosols are predominantly SO_4^{2-} and NO_3^- ; however there are also contributions from organic acids which have not been accounted for by the c/a (Kerminen et al., 2001). Base cations and NH_4^+ are involved in neutralizing acidic aerosols. A c/a near 1 indicates that the aerosols are generally neutral, whereas a lower ratio near 0.75 is indicative of acidic aerosols (Zhang et al., 2007; He et al., 2012). Daily c/a were determined only if all the ion measurements are available.

2.2.3 Scavenging ratio

In this study, monthly scavenging ratios (W) were first determined for ions existing only in the particulate phase (Ca^{2+} , Mg^{2+} , K^+ , Na^+ , and Cl^-) using Eq. 1 (Kasper-Giebl et al., 1998; He and Balasubramanian, 2008):

$$W = \frac{C_{prec}}{C_{air}} \times \frac{\rho_a}{\rho_w}, \quad (1)$$

C_{prec} and C_{air} are the precipitation and air concentrations, respectively. Surface air concentrations were used, even though in theory most of the scavenging occurs at the cloud height (Duce et al., 1991). ρ_a and ρ_w are the densities of air (1.2 kg m^{-3}) and water, respectively, which are used to convert the scavenging ratios to a mass basis. Scavenging ratios were determined on a monthly basis because they have less variability compared to daily (i.e. paired) or precipitation event scavenging ratios



(Galloway et al., 1993) and consider the average air concentration during both precipitation and dry periods (Kasper-Giebl et al., 1998). For the calculation of monthly scavenging ratios in Eq. 1, monthly volume-weighted precipitation concentrations and monthly average air concentrations based on ≥ 15 daily measurements in each month were used. Only daily precipitation concentrations with at least 0.2 mm precipitation amount were included. If there is insufficient data in each month, the scavenging ratio is not calculated. To account for the dependence on particle size distribution, the scavenging ratio of coarse PM (W_{cPM}) was determined by averaging W_{Ca} , W_{Mg} , and W_{Na} since these base cations are predominantly in coarse PM (Cheng et al., 2015). W_{K} was used as a surrogate for the scavenging ratio of fine PM (W_{fPM}) for inland sites, whereas $W_{\text{K}/2}$ was assumed for coastal sites following the methodology in Cheng et al. (2015). Scavenging ratios and wet scavenging in general are also affected by the chemical composition of aerosols, gas solubilities, temperature, precipitation amount and type, droplet size, nucleation efficiency, vertical concentration differences, and cloud type, which can contribute to the large variability in the scavenging ratios (Cadle et al., 1990; Duce et al., 1991; Galloway et al., 1993).

2.2.4 Relative contributions and scavenging ratios of gaseous and particulate phases

CAPMoN sites measure total NO_3^- , SO_4^{2-} , and NH_4^+ in precipitation. However, wet deposition of NO_3^- , SO_4^{2-} , and NH_4^+ can be attributed to the precipitation scavenging of particulates and gases, such as pNO_3^- and HNO_3 , pSO_4^{2-} and SO_2 , and pNH_4^+ and NH_3 (Kajino and Aikawa, 2015). To determine their relative contributions and the scavenging ratios of gases, particulate wet scavenging is first determined using W_{cPM} , W_{fPM} , particulate air concentration, and mass fractions in fine and coarse PM. The difference between the total wet scavenging and particulate wet scavenging is assumed to be due to the precipitation scavenging of gases. This assumption was also used in previous studies to estimate NO_3^- , HNO_3 , SO_4^{2-} , and SO_2 scavenging ratios (Cadle et al., 1990) and the wet scavenging contributions by gaseous oxidized mercury and particulate mercury (Sakata and Asakura, 2007; Cheng et al., 2015). Eq. 2 was used to determine the wet scavenging of pNO_3^- :

$$[\text{pNO}_3^-]_{\text{prec}} = W_{\text{fPM}} [\text{pNO}_3^-]_{\text{air}} P_f + W_{\text{cPM}} [\text{pNO}_3^-]_{\text{air}} (1 - P_f), \quad (2)$$

W_{fPM} and W_{cPM} are the monthly scavenging ratios of fine and coarse PM, respectively (Sect. 2.2.3). $[\text{pNO}_3^-]_{\text{air}}$ is the monthly average NO_3^- air concentration. P_f is the mass fraction of NO_3^- in fine PM, which varies with air mass origins and tends to form at lower temperatures (Zhang et al., 2008; Zhao and Gao, 2008). A P_f of 0.84 was assumed for the winter months (DJF), whereas 0.29 was used for all other months. These are average mass fractions observed at CAPMoN sites in a short-term field study (Zhang et al., 2008). Eq. 2 accounts for the different scavenging efficiencies of small and large particles.

The contribution of HNO_3 to nitrate wet deposition was calculated using Eq. 3:

$$[\text{HNO}_3]_{\text{prec}} = [\text{total NO}_3^-]_{\text{prec}} - [\text{pNO}_3^-]_{\text{prec}}, \quad (3)$$



[total NO₃⁻]_{prec} is the monthly volume-weighted NO₃⁻precipitation concentration and [pNO₃⁻]_{prec} is the wet scavenging of pNO₃⁻ calculated from Eq. 2. If [HNO₃]_{prec} < 0, it is assumed that only pNO₃⁻ contributed to total nitrate precipitation and no gas scavenging occurred. The relative contributions of particulate and gaseous species to NO₃⁻ wet deposition were determined using Eq. 4 and 5. Scavenging ratios of pNO₃⁻ and HNO₃ were determined using Eq. 1.

$$5 \quad \%pNO_3^- = ([pNO_3^-]_{prec} / [total\ NO_3^-]_{prec}) * 100\%, \quad (4)$$

$$\%HNO_3 = ([HNO_3]_{prec} / [total\ NO_3^-]_{prec}) * 100\%, \quad (5)$$

Similarly, Eq. 2-5 were used to determine the relative contributions of pSO₄²⁻ and SO₂ to total SO₄²⁻ wet deposition and pNH₄⁺ and NH₃ to total NH₄⁺ wet deposition. A P_f of 0.94 for [pSO₄²⁻]_{air} and P_f of 0.954 for [pNH₄⁺]_{air} was used for all months because these were the average mass fractions observed at CAPMoN sites (Zhang et al., 2008). pSO₄²⁻ and pNH₄⁺ have similar P_f because they have similar particle size distributions and often exist together as (NH₄)₂SO₄ in the atmosphere. Scavenging ratios for NH₃ were not determined because NH₃ air concentrations were not available.

3 Results and Discussion

3.1 Air concentrations

3.1.1 Geographical patterns

15 Air concentration statistics and geographical patterns of eight particulate inorganic ions, SO₂, and HNO₃ are plotted in Fig. 1a and b. The data were divided into two time periods from 1983-1996 and 1997-2010 to examine potential changes in concentrations due to NO_x and SO₂ emission changes. The range in concentrations (based on the 5th percentile to 95th percentile concentration) from all daily samples at all locations was 0.009-2.9 μg m⁻³ for Ca²⁺, 0.002-0.5 μg m⁻³ for Mg²⁺, and 0.006-0.2 μg m⁻³ for K⁺. Larger variability was observed in Ca²⁺ likely because of the variability of soil emissions depending on land use and wind. Large variability is also expected for Na⁺ and Cl⁻ because coastal sites are more frequently impacted by sea-salt aerosols than continental sites. The Na⁺ and Cl⁻ air concentrations ranged from 0.005-1.4 μg m⁻³ and 0.003-1.9 μg m⁻³, respectively. The range in concentrations were 0.018-5.8 μg m⁻³ for NH₄⁺, 0.009-8.7 μg m⁻³ for NO₃⁻, and 0.07-14.5 μg m⁻³ for SO₄²⁻. HNO₃ and SO₂ ranged from 0.014-5.0 μg m⁻³ and 0.011-25.2 μg m⁻³, respectively. These ions and trace gases are likely to have larger variability in air concentrations than base cations because some sites may be impacted more by anthropogenic emissions, which form secondary pollutants such as SO₄²⁻, HNO₃, NH₄⁺, and NO₃⁻, than other sites.

The geographical patterns in air concentrations were examined in greater detail based on the median concentration at each location. Long-term median Ca²⁺ concentrations among the sites ranged from 0.03-0.6 μg m⁻³. The highest median during both time periods were observed at Longwoods and Egbert, which are the lowest latitude and most inland air concentration



sites. Longwoods and Egbert are also predominantly agriculture sites. The median Mg^{2+} concentrations ranged from 0.01-0.09 $\mu g m^{-3}$. The highest median was also observed at Longwoods and Egbert. Higher median concentrations were also found at several western Canada sites including at Bratt's Lake, Esther and Saturna in the post-1997 period. The median concentrations ranged from 0.02-0.06 $\mu g m^{-3}$ for K^+ , which is the ion with the least spatial variability in the air concentration.

5 The highest concentrations were observed at Longwoods as well as at Bratt's Lake post-1997. The median Na^+ and Cl^- concentrations ranged from 0.02-0.5 $\mu g m^{-3}$ and 0.007-0.3 $\mu g m^{-3}$, respectively. As expected, the highest median for both ions were observed at the two coastal locations, Saturna and Kejimikujik, due to the proximity to sea-salt aerosol emissions from the ocean. These two sites are the farthest west and east air sampling locations respectively. Na^+ and Cl^- concentrations at Saturna were larger and had greater variability than at Kejimikujik likely because of the higher frequency of marine

10 airflows arriving at Saturna (68% of winds from N and W directions) than at Kejimikujik (31% of winds from E and S directions).

The median NH_4^+ and NO_3^- concentrations ranged from 0.1-1.7 $\mu g m^{-3}$ and 0.03-2.0 $\mu g m^{-3}$, respectively (Fig. 1a and b). Compared to pre-1997 period, the median concentrations of NH_4^+ and NO_3^- were lower in the post-1997 period. The highest concentrations for both ions were observed at Longwoods and Egbert. Higher concentrations were also found at Sutton,

15 Esther, and at Frelighsburg post-1997. The majority of these sites except for Sutton are agriculture sites located in southern Ontario and Quebec, which implies that higher ammonia emissions from agricultural regions may react with acidic gases in the atmosphere to form particulate ammonium (Pitchford et al. 2009). Acidic gases, such as H_2SO_4 and HNO_3 , are produced from the oxidation of SO_2 and NO_x respectively and are primarily emitted from industrial and urban areas. The proximity of these lower latitude air sampling sites to major industrial areas in Ohio and Pennsylvania, USA could result in higher acidic

20 gas concentrations at these sites. This is evident in the air concentration plots for HNO_3 that show higher concentrations of HNO_3 at sites having higher NO_3^- . The median HNO_3 concentrations ranged from 0.07-1.1 $\mu g m^{-3}$. Southerly winds also impacted Longwoods, Egbert, and Frelighsburg/Sutton approximately 20%, 32%, and 34% of the time, respectively. The median SO_4^{2-} concentrations among the air sampling sites ranged from 0.6-3.5 $\mu g m^{-3}$. The concentrations were lower during the post-1997 than during the pre-1997 period. The highest median concentration was observed at Longwoods.

25 Higher median concentrations were found at several southern Ontario and Quebec sites including Egbert, Sutton, Frelighsburg, Sprucedale, and Chalk River. Larger variability in the concentrations was generally observed across sites in southern and eastern Canada. This pattern is likely attributed to the proximity of the sites to combustion and industrial sources in southern Ontario and Quebec. The southern Canada and Atlantic Canada sites (e.g. Kejimikujik) are downwind of combustion and industrial areas in Ohio and Pennsylvania. In contrast, SO_4^{2-} concentrations at sites located in western and

30 central Canada (e.g., Saturna, Esther, Cree Lake, Bratt's Lake, and ELA) were at or below the overall median concentration of all the sites and had smaller variability.

The median SO_2 concentrations ranged from 0.4-6.4 $\mu g m^{-3}$ during the 1983-1996 period and from 0.6-2.3 $\mu g m^{-3}$ post-1997 (Fig. 1b). There was also a reduction in the variability of the concentrations in the post-1997 period. The lower latitude



southern Ontario and Quebec sites had higher SO_2 concentrations, whereas western and central Canada sites had much lower concentrations. This geographical pattern is similar to that of SO_4^{2-} . One exception was that the SO_2 concentrations in eastern Canada were similar to or even lower than in western Canada, whereas SO_4^{2-} concentrations in eastern Canada were slightly higher than in western Canada. Eastern Canada sites including Montmorency, Lac Edouard, and Kejimikujik are remote sites; therefore SO_2 concentrations are likely not elevated by the time it arrives at these remote locations since SO_2 can undergo deposition or transform to SO_4^{2-} during transport. The slightly higher SO_4^{2-} in eastern Canada could be from sea-salt sulfate due to the proximity to the Atlantic Ocean.

3.1.2 Temporal patterns

The Kendall slopes and confidence interval in Table 2 shows the annual rate of change in the concentrations of particulate ions and trace gases at the air sampling sites for all years with available data. A significant temporal trend in Ca^{2+} was observed at 5 of 16 sites with no significant changes in the concentrations observed at the remaining sites. Decreasing trends were observed at Saturna, Longwoods, and Egbert, while increasing trends were observed at Esther and Kejimikujik. The largest decline in Ca^{2+} was $-16 \text{ ng m}^{-3} \text{ a}^{-1}$ at Longwoods. Overall the temporal changes in Ca^{2+} are small. For Mg^{2+} , a significant decreasing trend was found at Saturna, Longwoods, Chalk River, and Kejimikujik. However, the rate of decline was very small ranging only from -0.5 to $-1.1 \text{ ng m}^{-3} \text{ a}^{-1}$. The rate of decline for K^+ ranged from -0.5 to $-3.8 \text{ ng m}^{-3} \text{ a}^{-1}$ and was observed at 14 of 16 sites. A plot of the annual average K^+ for ten of the active air sampling sites are shown in Fig. 2a for the 1983-2010 period, which illustrates a gradual decline in K^+ . Significant decreases in Na^+ were found at 11 of 16 sites with magnitudes ranging from -0.3 to $-4.5 \text{ ng m}^{-3} \text{ a}^{-1}$. The steepest decline was observed at a coastal site in western Canada. However, increasing trends were observed at two coastal sites in eastern Canada (Montmorency and Kejimikujik). For Cl^- , decreasing temporal trends were found at only 6 of 16 sites, suggesting that the temporal trends are not necessarily related to sea-salt emissions. The decline in Cl^- , ranging from -0.1 to $-0.8 \text{ ng m}^{-3} \text{ a}^{-1}$, were found at sites in western and central Canada and at Algoma and Longwoods.

NH_4^+ concentrations have been decreasing at 12 of 16 air sampling sites (Table 2). This result is consistent with the widespread decrease in NH_4^+ at CAPMoN sites during 1988-2007 (Zbieranowski and Aherne, 2011). The rate of decrease ranged from -4 to $-58 \text{ ng m}^{-3} \text{ a}^{-1}$. The largest declines as shown in Fig. 2b were observed at Longwoods, Egbert, Sprucedale, and Frelighsburg, which are agriculture sites located in southern Ontario and Quebec. The annual decrease was 7.3 times greater than other sites based on the linear regression slopes. The decreasing trend in NH_4^+ corresponds to the decreasing trend in ammonia emissions in Ontario and Quebec particularly in the post-2002 period (Fig. 2b) (Environment Canada, 2014). Aside from its relationship to ammonia, the negative trend in NH_4^+ was also strongly tied to trends in NO_3^- and SO_4^{2-} . There was an even split in the number of sites with increasing trends and decreasing trends in NO_3^- . The rate of increase ranged from 1.3 - $6.4 \text{ ng m}^{-3} \text{ a}^{-1}$ among active sites, whereas the annual trend was 6 - $40 \text{ ng m}^{-3} \text{ a}^{-1}$ among inactive sites (e.g. Esther, Sutton, Montmorency). The annual trend in NO_3^- decreased from -9.3 to $-53 \text{ ng m}^{-3} \text{ a}^{-1}$ at other sites (Table 2).



Larger declines were observed at the agriculture sites located in southern Ontario and Quebec. Differences in temporal trends were also observed during different time periods. At 9 of 16 sites, an increasing trend was found between 1991 and 2001 which was followed by a decreasing trend from 2001 to 2010 (Fig. 3). The difference in NO_3^- trends between the two decades was also reported in previous analysis of CAPMoN sites (Zbieranowski and Aherne, 2011). The change in NO_3^- temporal trends closely resembled that of NO_x emissions in Canada. Between 1991 and 1997, NO_x emissions in Canada increased annually and only began to decrease from 1997 to 2010 (Fig. 3) (Environment Canada, 2014). In the U.S., NO_x emissions were constant over the 1991-1994 period and only began to decrease after 1994 (USEPA, 2015). Reductions in NO_x emissions were implemented following the introduction of the Canada-U.S. Air Quality Agreement and the U.S. Acid Rain Program and Clean Air Interstate Rule. The decrease in NO_x emissions were largely attributed to lower emissions from stationary fuel combustion and transportation sectors (Lloret and Valiela, 2016).

SO_4^{2-} decreased at a rate of -28 to -109 $\text{ng m}^{-3} \text{a}^{-1}$ depending on the location (Table 2). The steepest annual declines were observed in the southern Ontario and Quebec region as shown in Fig. 4. The slope of the linear regression equation for the southern Ontario and Quebec sites in Fig. 4 was two times greater than that of other air sampling sites, which are coastal or higher latitude sites distant from major industrial and urban areas. The geographical patterns in the temporal trends of SO_4^{2-} were also similar to those of SO_2 and HNO_3 . The annual trends for SO_2 and HNO_3 in the southern Ontario and Quebec region declined 3.8 and 4.9 times faster, respectively, than other air sampling sites across Canada based on the linear regression slopes. Negative trends for SO_4^{2-} and SO_2 concentrations followed the decreasing trend in SO_2 emissions in both Canada and U.S. since 1990 (Environment Canada, 2014; USEPA, 2015) (Fig. 4), corresponding to the period of the Canada-U.S. Air Quality Agreement and the U.S. Acid Rain Program and Clean Air Interstate Rule. Note the steeper decline in SO_2 emissions in Ontario in recent years, which is potentially attributed to the phase-out of coal use in Ontario power plants beginning in 2005 (MOE, 2015).

The influence of meteorological parameters including temperature, relative humidity and precipitation rates on the temporal trends of particulate ions and trace gases were also investigated by performing correlation analyses on the monthly averaged data. The descending trend in K^+ between 1993 and 2010 at the majority of the sites was not strongly influenced by precipitation as evident by the weak correlation coefficients (Table S1). Higher correlation between monthly average K^+ and temperature were found at Sprucedale, Frelighsburg and Lac Edouard ($r = 0.52-0.69$, $p < 0.05$). At these sites, the monthly average K^+ peaked in March-April and was at the minimum concentration during December-January, which resembled the seasonal temperature cycle (Fig. S2a). The higher K^+ in the early spring could be attributed to increase soil emissions from agriculture operations and forest fires during springtime since the major sources of particulate K^+ are from biomass and soil. Decreasing NH_4^+ observed at most of the sites was only weakly correlated with monthly precipitation rates and relative humidity, implying these meteorological parameters had little influence on the long-term temporal trend. Higher correlation between monthly average NH_4^+ and temperature was found at Kejimikujik ($r = 0.63$, $p < 0.05$). The maximum NH_4^+ typically occurred during April-May and reached its lowest concentration during December-January (Fig. S2b). This seasonal trend is



linked to the formation of SO_4^{2-} through SO_2 oxidation, which tends to occur at higher temperatures because of increase production of atmospheric oxidants. This theory is consistent with the very high correlation between monthly average NH_4^+ and SO_4^{2-} ($r = 0.91$, $p < 0.05$) at Kejimikujik. Overall, strong correlations between NH_4^+ and SO_4^{2-} were observed at all the sites ($r = 0.6$ - 0.94 , $p < 0.05$). The high correlation between $\text{SO}_4^{2-}/\text{SO}_2$ ratio and temperature ($r = 0.61$ - 0.84 , $p < 0.05$) suggests SO_4^{2-} formation from the gas-phase oxidation of SO_2 (Yao et al., 2002). Besides the relationship between NH_4^+ and SO_4^{2-} , three of the sites including Saturna, ELA and Egbert exhibited strong correlations between NH_4^+ and NO_3^- ($r = 0.52$ - 0.7 , $p < 0.05$) indicating that NH_4^+ also followed the temporal trend of NO_3^- at some locations. In summary, precipitation and relative humidity had little impact on the long-term temporal patterns of particulate ions. Seasonal temperature trends is linked with the seasonal cycle of atmospheric oxidants which explains the short-term patterns in SO_4^{2-} and NH_4^+ ; however, there is no clear evidence that long-term temperature changes impacted their long-term trends.

3.1.3 Aerosol acidity (c/a)

The median c/a ranged from 0.97-1.6 and an overall median c/a of 1.07 was observed across all sites (Fig. 5a). These values are based on inorganic ion contributions to aerosol acidity. Organic acids do not contribute significantly to aerosol acidity compared to the strong inorganic acids (Zhang et al., 2007; Ziemba et al., 2007; He et al., 2012); however, they have been included in the measure of aerosol acidity in some studies (Hennigan et al., 2015 and references therein). Among the sites, the highest aerosol acidity was observed at Kejimikujik because of the higher equivalent anion concentrations relative to cations. Higher aerosol acidity was prevalent generally in eastern Canada and central Ontario regions. In contrast to Kejimikujik, the majority of the sites had higher cation than anion concentrations or near equivalent cation and anion concentrations. Even though locations like Longwoods and Egbert had greater amount of anions than other locations due to higher NO_3^- and SO_4^{2-} , there were sufficient amounts of cations, mainly NH_4^+ , to neutralize the acidic species. While the overall median c/a was close to 1 for all Canadian sites, more than half of the daily c/a data were below 1 at eight locations (Fig. 5a). This suggests there was a substantial amount of time between 1994 and 2010 when aerosols were acidic at some Canadian sites.

A significant increasing trend in the c/a was observed between 1994 and 2010, which indicates a widespread decline in aerosol acidity (Fig. 5b). The rate of decrease in aerosol acidity was small and fairly uniform spatially based on the Kendall slope results. According to Fig. 5b, the annual average cation and anion concentrations and c/a at most of the sites (data combined from 13 of 15 sites) were relatively constant between 1994 and 2000. Since 2001, the annual average cation and anion concentrations and aerosol acidity have been on a slight decline. The decrease in cation concentrations appeared consistent with the declining trend in NH_4^+ discussed earlier, since NH_4^+ is the largest contributor to cation concentrations. For anions, NO_3^- and SO_4^{2-} are the predominant ions. Thus, the decline in anions was also consistent with the decreasing rates for NO_3^- and SO_4^{2-} . As mentioned earlier, the decreasing trends in NH_4^+ , NO_3^- and SO_4^{2-} were consistent with the reductions in ammonia, NO_x and SO_2 emissions.



3.2 Wet deposition

3.2.1 Geographical patterns

The annual wet deposition statistics for the various ions at the 30 locations are shown in Fig. 6. The annual wet deposition was based on all years with complete data because the annual flux was determined by summing the daily fluxes. The range in the annual wet deposition based on the 5th and 95th percentile annual wet deposition rate ($\text{kg ha}^{-1} \text{a}^{-1}$) was: 0.08-3.6 for Ca^{2+} , 0.02-1.6 for Mg^{2+} , 0.01-0.7 for K^+ , 0.03-12.0 for Na^+ , 0.06-23.0 for Cl^- , 0.1-6.4 for NH_4^+ , 0.4-26.5 for NO_3^- , and 0.5-32.7 for SO_4^{2-} . The lowest annual wet deposition rates for Ca^{2+} , Mg^{2+} , Na^+ , NH_4^+ , NO_3^- , and SO_4^{2-} were observed at Snare Rapids, which is a remote site in the Northwest Territories of Canada. The highest annual wet deposition recorded at the most eastern coastal site in Bay d'Espoir, Newfoundland were from ions related to sea-salt aerosols, including Na^+ , Cl^- , and Mg^{2+} . For Ca^{2+} and ions derived from anthropogenic sources (e.g., NH_4^+ , NO_3^- , and SO_4^{2-}), the highest annual wet deposition rates were observed at Priceville and Longwoods, which are the two most southern wet deposition sites in Canada and closest to urban and industrial areas.

Long-term median annual wet deposition of Ca^{2+} ranged from 0.1-2.8 $\text{kg ha}^{-1} \text{a}^{-1}$ among the wet deposition sites. The highest annual wet deposition was observed at Priceville and Longwoods (Fig. 6). Higher median wet deposition was also found at Algoma, Egbert, and Warsaw Caves. The majority of these sites are agriculture sites. The lowest median wet deposition was observed at the western and eastern coastal sites. The median annual wet deposition of Mg^{2+} ranged from 0.03-1.0 $\text{kg ha}^{-1} \text{a}^{-1}$. The highest wet deposition was found at the western and eastern coastal sites with the exception of Goose Bay, which is a higher latitude coastal site located in Labrador. It had the lowest annual precipitation amount among coastal sites in eastern Canada (Fig. S3). Annual Mg^{2+} wet deposition at inland sites was typically at or below the overall median wet deposition for all sites; however, they are slightly higher at Longwoods and Priceville. The median annual wet deposition of K^+ ranged from 0.05-0.4 $\text{kg ha}^{-1} \text{a}^{-1}$. Similar to Mg^{2+} , higher annual wet deposition of K^+ was observed at eastern coastal locations with the exception of Goose Bay. Annual wet deposition for inland sites was around the overall median annual wet deposition for all sites except at Longwoods, Algoma and Priceville. The median annual wet deposition of Na^+ and Cl^- ranged from 0.05-7.5 $\text{kg ha}^{-1} \text{a}^{-1}$ and 0.1-13.6 $\text{kg ha}^{-1} \text{a}^{-1}$, respectively. The geographical patterns in the annual wet deposition were similar between Na^+ and Cl^- . Annual wet deposition at western and eastern coastal sites were higher and had greater variability than inland locations.

Median annual NH_4^+ wet deposition ranged from 0.2-5.8 $\text{kg ha}^{-1} \text{a}^{-1}$ (Fig. 6). Higher annual wet deposition was observed at lower latitude continental sites. Higher latitude continental locations (e.g. Cree Lake, Island Lake, Pickle Lake, Bonner Lake, Chapais) and coastal locations were well below the overall median annual wet deposition. The median annual wet deposition ranged from 0.8-23.3 $\text{kg ha}^{-1} \text{a}^{-1}$ for NO_3^- and 0.8-26.6 $\text{kg ha}^{-1} \text{a}^{-1}$ for SO_4^{2-} . These two ions have similar spatial patterns in annual wet deposition. Higher median annual wet deposition occurred at southern Ontario and Quebec sites. Lower median annual wet deposition was observed in eastern Canada. The lowest median annual wet deposition for NO_3^-



and SO_4^{2-} , which were well below the overall median annual wet deposition for all sites, was recorded in western and central Canada.

The geographical patterns in the wet deposition were predominantly affected by the air concentrations. For example, the higher Na^+ and Cl^- wet deposition at coastal locations can be traced back to the higher Na^+ and Cl^- air concentrations. Similarly, the higher NH_4^+ , NO_3^- and SO_4^{2-} wet deposition occurring at southern Ontario and Quebec locations was consistent with the geographical patterns in the air concentrations. Although precipitation amount is used to determine wet deposition, only the wet deposition patterns of Mg^{2+} and K^+ were potentially influenced by precipitation amount. As shown in Fig. S3, the annual precipitation amount generally increases from western to eastern sites. Only the Mg^{2+} and K^+ wet deposition were higher at eastern Canada locations.

10 3.2.2 Temporal trends

Long-term temporal trends in the annual wet deposition of ions were analyzed using Sen's slope (Table 3 and 4) and linear regression analysis. The annual wet deposition of Ca^{2+} and K^+ has not changed significantly at almost all locations. For Mg^{2+} and Na^+ , there were no significant changes in the annual wet deposition rate at most of the sites, while a very small statistically significant decline in the annual wet deposition was observed at other sites. Of these sites, the rate of decline ranged from -0.001 to $-0.008 \text{ kg ha}^{-1} \text{ a}^{-1}$ for Mg^{2+} and -0.002 to $-0.02 \text{ kg ha}^{-1} \text{ a}^{-1}$ for Na^+ . Decline in base cations has been reported at other Canadian sites during the 1990s (Watmough et al., 2005). The small decrease or lack of change in base cation wet deposition is expected because the major source of base cations at rural Canadian sites are from natural emissions (Watmough et al., 2005). Monitoring the wet deposition Ca^{2+} , Mg^{2+} , K^+ , and Na^+ trends are important because these ions neutralize soil acidity and mitigate further harmful impacts to plants and wildlife. A declining trend in the Cl^- wet deposition was observed at 5 of 16 sites (Fig. 7a), and the magnitude ranged from -0.007 to $-0.03 \text{ kg ha}^{-1} \text{ a}^{-1}$ (Table 3).

Significant trends in the annual wet deposition of NH_4^+ were observed at only 3 of 16 locations. There were two sites with increasing temporal trend ($0.05 \text{ kg ha}^{-1} \text{ a}^{-1}$), whereas a decreasing trend was found at one location (Table 4). A lack of an overall consistent temporal trend in precipitation NH_4^+ was also found in previous analysis of CAPMoN sites (Zbieranowski and Aherne, 2011). These trends were in contrast to those in the U.S., which has seen an increase in precipitation NH_4^+ at 64% of the wet deposition sites between 1985 and 2004 (Lehmann et al., 2007). While increasing NH_4^+ in precipitation helps to increase precipitation pH and promote plant growth, a counter-effect is that soils can become acidic when NH_4^+ undergoes nitrification (Vogt et al., 2006).

Declining trends in NO_3^- wet deposition was observed at 10 of 16 sites (data combined in Fig. 7a), while no significant trend was found at other locations. The rate of decrease ranged from -0.07 to $-1.0 \text{ kg ha}^{-1} \text{ a}^{-1}$ and was largest at the southern Ontario and Quebec sites (Algoma, Longwoods, Egbert, Sprucedale, Frelighsburg, Lac Edouard). One exception was the non-significant trend at Sutton (Table 4) even though this site is only 15 km from Frelighsburg. The discrepancy in the



temporal trends at these two sites can be partially attributed to the different measurement periods. Measurements of wet deposition at Sutton ended in 2002, whereas Frelighsburg has been actively measuring wet deposition since 2001. This suggests the rate of decrease in NO_3^- wet deposition was more rapid in the period after 2001 and corresponds with the decline in NO_3^- air concentrations over the same time period discussed earlier. In the U.S. northeast, the decline in precipitation NO_3^- was observed at only 25% of the sites in that region during 1985-2004 (Lehmann et al., 2005). A recent study of NO_3^- wet deposition from 1985-2011 across North America indicates a 40-50% decrease in eastern North America after 2000 (Lloret and Valiela, 2016). Similar to the air concentrations of SO_4^{2-} , decline in SO_4^{2-} wet deposition was also prevalent throughout Canadian sites. This finding is consistent with the decrease in precipitation SO_4^{2-} reported at other Canadian sites during the 1990s (Watmough et al., 2005) and at 89% of the wet deposition sites in the U.S. between 1985 and 2004 (Lehmann et al., 2007). Decreasing temporal trends in SO_4^{2-} wet deposition was found at 11 of 16 sites with magnitudes ranging from -0.1 to $-1.0 \text{ kg ha}^{-1} \text{ a}^{-1}$ depending on the location (Table 4). The overall rate of decline was ~ 2 times higher at the southern Ontario and Quebec sites relative to other locations (Fig. 7b), which is consistent with the patterns in the air concentrations of SO_4^{2-} described earlier. The large declining trends in the wet deposition of nitrogen and sulfur-containing species in conjunction with the relatively smaller declines or lack of change in base cations indicate that acid rain has attenuated over time. This is largely attributed to policies controlling NO_x and SO_2 emissions.

Daily wet deposition of ions was correlated with their respective daily particulate matter concentrations and daily precipitation amount to gain insight into factors influencing the temporal trends in wet deposition. Moderate correlations ($r = 0.38-0.41$, $p < 0.05$) between daily wet deposition and particulate matter concentration were found for SO_4^{2-} , Na^+ and Cl^- , whereas only weak correlations were found for other ions. This result partly explains the prevalent decline in wet deposition of SO_4^{2-} and Cl^- . Decreasing NO_3^- wet deposition was also widespread; however it did not strongly correlate with particulate NO_3^- concentrations ($r = 0.21$, $p < 0.05$). This is potentially because both gaseous and particulate nitrogen species can contribute to NO_3^- wet deposition. This is supported by the slightly higher correlation ($r = 0.33$, $p < 0.05$) between daily NO_3^- wet deposition and HNO_3 . For SO_4^{2-} wet deposition which can be attributed to the precipitation scavenging of particulate SO_4^{2-} and SO_2 , only a weak correlation was found between daily SO_4^{2-} wet deposition and SO_2 ($r = 0.13$, $p < 0.05$). Further analysis on the relative contributions of gaseous and particulate species to NO_3^- and SO_4^{2-} wet deposition will be discussed in Sect. 3.4. Moderate correlations between daily wet deposition and daily precipitation were found for NH_4^+ , NO_3^- and SO_4^{2-} ($r = 0.50-0.56$, $p < 0.05$), while weaker correlations were found for other ions. Some correlation was expected because wet deposition is determined from precipitation concentration and precipitation amount. On an annual basis, there has been no significant change to the annual precipitation amount at most of the sites, except for significant increases at Bratt's Lake, ELA, Chalk River, and Kejimikujik (Table 4). The lack of change to the annual precipitation is inconsistent with the decreasing trends in SO_4^{2-} , NO_3^- and Cl^- annual wet deposition found at the majority of the sites. Thus, long-term wet deposition of ions was not strongly influenced by long-term precipitation trends between 1983 and 2010.



3.2.3 Acid rain

The geographical patterns in acid rain as measured by precipitation pH are shown in Fig. 8. Precipitation pH is slightly acidic by nature due to the presence of carbonic acid formed by the dissolution of CO₂. A pH below 5 is considered to be acidic precipitation (Lehmann et al., 2007). According to Fig. 8, the median pH in daily precipitation samples across the sites ranged from 4.4-5.7. Between 1983 and 2011, acidic precipitation was observed in more than 50% of the daily precipitation samples at 19 of 31 or 61% of the sites. Acidic precipitation was prevalent in southern Ontario and some parts of eastern Canada, whereas pH was above 5 in western and central Canada. Similarly in regions close to southern Ontario and eastern Canada, higher occurrences of acid rain have been observed in the U.S. northeast region during the 1994-1996 and 2002-2004 periods (Lehmann et al., 2007). Acid rain has contributed to the acidification of soil and lakes (Stoddard et al., 1999; Driscoll et al., 2001; Clair et al., 2002; 2003; Jeffries et al., 2003; Watmough and Dillon, 2003). In the southern Ontario and eastern Canada region, the acid deposition effects are more concerning because the soil is slightly acidic naturally and shallow and the underlying bedrock provides insufficient acid buffering capacity (Clair et al., 2002; Watmough and Dillon, 2003). The geographical patterns in precipitation pH were consistent with those of aerosol acidity discussed earlier. The correlation between the median pH and aerosol acidity (as measured by c/a ratio) among 15 locations was 0.68, which suggests acidic particles partially contributed to acid rain at various Canadian sites.

Between 1983 and 2011, an increasing trend in pH was observed at 13 of 16 sites, while no significant change in pH was found at the remaining three sites (Table 4). The overall decline in acidic precipitation in Canada is consistent with the trends in the U.S. (Lehmann et al., 2007). The rate of increase in pH was slightly higher at southern Ontario and Quebec sites (Table 4). Recent studies indicate there has been a gradual improvement to soil and surface water conditions due to decreases in NO₃⁻ and SO₄²⁻ wet deposition; however, this recovery has been outpaced by the rate of decline in acidic wet deposition (Strock et al., 2014; Lawrence et al., 2015). The increasing temporal trends in pH can be partially attributed to aerosol acidity. A correlation of 0.29 between daily pH and c/a was found in this study. Based on the annual trend between the 1994 and 2010 period, the annual average pH and c/a (data combined at 13 of 15 sites) had very similar trends (Fig. 5b) and the correlation coefficient improved to 0.86.

3.3 Scavenging ratios

3.3.1 General statistics and comparisons with literature

A summary of the monthly average scavenging ratio (*W*) (on a mass basis) statistics for the inorganic ions and trace gases are provided in Table S2. Monthly *W*_{Ca} ranged from 120-14338. The minimum and maximum values were found at Egbert and Algoma, respectively. *W*_{Mg} ranged from 131-11243. The lowest *W* was recorded at Chapais, while the highest *W* was recorded at Kejimikujik. *W*_{Na} ranged from 76-12165. The lowest *W* was recorded at Chapais, while the highest *W* was recorded at Kejimikujik similar to Mg²⁺. The *W*_K ranged from 69-5565 and had lower values compared to Ca²⁺, Mg²⁺, and



- Na⁺ because K⁺ is predominantly in fine particulate matter except for an additional coarse mode found at coastal locations (Zhang et al., 2008). For this reason, it is assumed that the W of fine PM (W_{fPM}) was equivalent to the W_K for inland sites, while W_{K2} was assumed for coastal sites. The minimum and maximum W_K were found at Montmorency and Kejimikujik, respectively. Since Ca²⁺, Mg²⁺, and Na⁺ are mainly associated with coarse particulate matter, the average W of these ions was used as an estimate of the W of coarse particles (W_{cPM}). The range of W_{cPM} was 83-12165. The minimum and maximum values were found at Chapais and Kejimikujik, respectively. The W_{Cl} ranged from 210-35521. The minimum and maximum values were found at Chapais and Algoma, respectively. Compared to other ions, W_{Cl} were larger and had greater variability. Overall, the range in the average W for these ions among the 13 sites was within the average W from previous studies (Table S3).
- 10 Monthly scavenging ratios were determined for particulate NO₃⁻ (pNO_3^-) and HNO₃ separately because both gaseous and particulate forms can contribute to NO₃⁻ wet deposition. Monthly W ranged from 135-4272 for pNO_3^- and 7-16658 for HNO₃. Based on the average scavenging ratio, W_{HNO_3} were greater than W_{pNO_3} . The average W_{pNO_3} from 13 sites were within the range of literature values in Table S3; however the majority of the W_{pNO_3} in the literature are determined from total nitrate in precipitation and pNO_3^- in air. Thus, most of the W_{pNO_3} are overestimated. Scavenging ratios of pNO_3^- based on
- 15 total nitrate in precipitation are higher by a factor of 1.4-18 depending on the site (average: factor of 6).
- In this study, the average W_{HNO_3} at some sites were higher than those in Table S3; however, they were most comparable to the average determined by Cadle et al. (1990) likely because of the similarity in the methods of determining W_{HNO_3} . The method first calculates the pNO_3^- scavenged and then the difference between the total NO₃⁻ and the pNO_3^- scavenged is assumed to be contributed by HNO₃ scavenging. One major difference in the approach was that Cadle et al. (1990) used W_K
- 20 as a surrogate for W_{pNO_3} to estimate the pNO_3^- scavenged, whereas in this study W_{pNO_3} considered the seasonal particle size distribution of pNO_3^- . The average W_{HNO_3} at some sites in this study were different than those determined by Hicks (2005) (Table S3), who assumed only HNO₃ contributed to NO₃⁻ wet deposition. The values were also different from that of Kasper-Giebl et al. (1998), who used a multiple linear regression (MLR) approach. For comparison purposes, W_{pNO_3} and W_{HNO_3} derived from MLR are also shown in Table S3 and S4. The MLR results show $W_{HNO_3} > W_{pNO_3}$. However, this
- 25 empirical method generated higher W_{pNO_3} and lower W_{HNO_3} at some locations compared to the method used in this study. Table S4 indicates that the MLR model fit was considered weak to moderate ($R^2 = 0.15-0.34$) depending on the site.
- Monthly W_{pNH_4} ranged from 63-4356. The lowest W was recorded at Egbert, while the highest W was recorded at Algoma. Scavenging ratios of NH₃ were undetermined because NH₃ air concentrations were not available. Average W_{pNH_4} were also lower than some of the values in the literature (Table S3), which are likely overestimated because the values were based on
- 30 the total NH₄⁺ precipitation concentrations, instead of pNH_4^+ scavenged by precipitation. Comparison of these two methods of calculation indicates that the use of total NH₄⁺ precipitation concentration overestimated the scavenging ratios by 4-48% (average: 22%) depending on the location. Despite the coexistence of NH₄⁺ and SO₄²⁻ in the atmosphere, the difference



between the average scavenging ratios of these ions can vary by 4-98% (average: 32%). The range of monthly scavenging ratios for pSO_4^{2-} and SO_2 were 75-3146 and 0.3-12068, respectively. The average W_{pSO_4} among the sites in this study were lower than some of the literature values in Table S3. Most of the studies excluded the wet scavenging of SO_2 because pSO_4^{2-} was assumed to be the dominant contributor to SO_4^{2-} wet deposition. This method overestimates the scavenging ratio of pSO_4^{2-} by 18-85% (average: 44%) compared to the method used in this study. According to the limited number of W_{SO_2} estimates (Table S3), the precipitation scavenging of SO_2 is less important compared to pSO_4^{2-} because of the lower W_{SO_2} . In this study, SO_2 and pSO_4^{2-} can be equally important at times in terms of scavenging ratios. The average W_{SO_2} at more than half of the sites in this study were greater than literature averages. This is potentially due to the different methodologies for calculating W_{SO_2} and precipitation type. The MLR method yielded higher W_{pSO_4} and lower W_{SO_2} at some locations compared to the method used in this study (Table S3 and S4). The approach used in this study was similar to Cadle et al. (1990); however, that study used W_{NH_4} as a surrogate for W_{pSO_4} based on the assumption these ions are typically found in the same aerosols. There are however large uncertainties with W_{NH_4} because of the scavenging by both pNH_4^+ and NH_3 . As mentioned earlier, most of the W_{NH_4} in literature are overestimated because of the exclusion of NH_3 . Use of these values could lead to a high bias in W_{pSO_4} and subsequently lower W_{SO_2} . Aside from the methodology, the scavenging ratios determined by Cadle et al. (1990) were based on snowfall events, which favor the scavenging of particles over gases (Hicks, 2005; Zhang et al., 2013; 2015).

The variability in scavenging ratios among different ions and trace gases within the same month is shown in Fig. S4. The range in scavenging ratios can be quite large. This is expected because the different physical and chemical properties of the pollutants affect their wet scavenging efficiencies. For particulate matter, coarse particles (e.g., Ca^{2+} , Mg^{2+} and Na^+) are scavenged more efficiently than fine particles (e.g. K^+) (Galloway et al., 1993; Guerzoni et al., 1995; Tuncel and Ungör, 1996). The different solubilities of gaseous pollutants (HNO_3 and SO_2) can also explain the differences in scavenging ratios for different pollutants. W_{HNO_3} were 1.4 to 6 times higher than those of W_{SO_2} depending on the location (Table S2), which is consistent with the higher solubility of HNO_3 compared to SO_2 ($H = 2.1 \times 10^5 \text{ M atm}^{-1}$ vs. 1.2 M atm^{-1} ; Zhang et al., 2006; Sander, 2015).

3.3.2 Patterns in scavenging ratios

Although the monthly scavenging ratios of most ions span a wide range, the average scavenging ratios of particulate ions were within a factor of 1.6-4.5 among the 13 sites (Table S2). The average scavenging ratios of Na^+ , Cl^- and Ca^{2+} have larger spatial variability than other particulate ions. This may reflect the different precipitation scavenging efficiencies of particles in the marine boundary layer and continental atmospheres as hypothesized by Galloway et al. (1993). One related theory is that the higher relative humidity in marine environments is conducive to the hygroscopic growth of sea-salt aerosols which increases its scavenging efficiency (Hennigan et al., 2008). The average scavenging ratios ranged from 497-996 for fine particles (factor of 2 spatial variability) and 666-2077 for coarse particles (factor of 3 spatial variability). Larger



scavenging ratios of fine particles were found at inland sites, where soil and biomass emissions are sources of K^+ . For coarse particles, the larger scavenging ratios at coastal sites (Table S2) were likely attributed to oceanic source of Na^+ and Mg^{2+} . The greatest spatial variability was in the scavenging ratios of gases including HNO_3 and SO_2 . The average scavenging ratios varied by a factor 7.4 and 10.7, respectively. The large variability in scavenging ratios between sites is expected because the air and precipitation concentrations and precipitation type and amounts among other factors can also vary with location.

A pronounced seasonal variation can be seen in the monthly average scavenging ratios. The average scavenging ratio of most of the ions and HNO_3 were lowest during July or August (Fig. S5), which resembles the monthly NO_3^- , SO_4^{2-} , and NH_4^+ trends in a previous study (Kasper-Giebl et al., 1998). There were two periods when the average scavenging ratios peaked: one peak during April-May and a second peak during September-October were observed for most of the ions and HNO_3 . A similar pattern was obtained for W_{pNO_3} when MLR was used to generate monthly scavenging ratios. However, different patterns were obtained for W_{HNO_3} and W_{pSO_4} derived from MLR, as shown by the higher values during winter and lower values in the warm seasons (Fig. S5 and Table S5).

Monthly patterns in W_{SO_2} were different from those of other ions and HNO_3 . The average W_{SO_2} were lower during winter and peaked in the summer, and is supported by the MLR results as well (Fig. S5 and Table S5). This result is also consistent with the seasonal W_{SO_2} patterns from multiple U.S. sites (Hicks, 2005) and other studies suggesting the inefficient scavenging of SO_2 by snow (Kasper-Giebl et al., 1998 and references therein). However, limited field measurements of dissolved SO_2 (measured as sulfite) in precipitation samples indicate that the highest precipitation concentrations were found in the colder months, which is consistent with solubility theory (Hales and Dana, 1979; Dana, 1980). This finding does not necessarily contradict the results from this study because W_{SO_2} also depend on the air concentration. The higher ambient SO_2 likely due to higher combustion emissions associated with winter heating (Fig. S6) resulted in lower scavenging ratios, and vice-versa during warmer months. Besides temperature effects on solubility, precipitation pH and the presence of NH_3 and H_2O_2 could also affect SO_2 wet scavenging (Zhang et al., 2006).

3.4 Relative contributions of particulates and gases to nitrate, ammonium and sulfate wet deposition

In the previous section, scavenging ratios were determined for particulate (pNO_3^- , pNH_4^+ , pSO_4^{2-}) and gaseous (HNO_3 and SO_2) species. In this section, the relative percent contributions of these particulate and gaseous species to nitrate, ammonium, and sulfate wet deposition are determined. The average $\pm 1\sigma$ of pNO_3^- contributions to nitrate wet scavenging ($\%pNO_3^-$) was $28\pm 23\%$ for all years of data at the 13 locations. Percent HNO_3 contributions to nitrate wet scavenging ($\%HNO_3$) was $72\pm 23\%$. Based on the average, $\%HNO_3$ dominated $\%pNO_3^-$ at most of the sites (Fig. 9a). Geographical variations were observed in the $\%pNO_3^-$ and $\%HNO_3$. Average $\%pNO_3^-$ were higher at the two lowest latitude sites and coastal sites (Fig. 9a). One reason is because of the higher pNO_3^- air concentrations at the lower latitude locations (Longwoods and Egbert) discussed in Sect. 3.1.1. $\%pNO_3^-$ were also higher at the coastal locations (Saturna and



Kejimkujik) likely because of the partitioning of HNO_3 to sea-salt aerosols (Pryor and Sørensen, 2000; Fischer et al., 2006), which are typically coarse particles and hygroscopic and hence more efficiently removed by precipitation. In contrast, $\% \text{HNO}_3$ were greater at the higher latitude continental locations (Fig. 9a). Relative contributions of pNH_4^+ and NH_3 were $70 \pm 19\%$ and $30 \pm 19\%$, respectively. Precipitation scavenging of pNH_4^+ was greater than NH_3 at all sites (Fig. 9b). The percent pSO_4^{2-} contributions to sulfate wet scavenging ($\% \text{pSO}_4^{2-}$) was $63 \pm 20\%$, while percent SO_2 contributions to sulfate wet scavenging ($\% \text{SO}_2$) was $37 \pm 20\%$. Average $\% \text{pSO}_4^{2-}$ were greater than that of $\% \text{SO}_2$ at most of the sites (Fig. 9c). No pronounced geographical patterns were observed in the relative contributions of gases and particulates to ammonium or sulfate wet deposition. Knowledge of the relative scavenging contributions of gases and particles may improve the wet deposition modeling of nitrate, ammonium, and sulfate, which continues to show discrepancies between model and observations (Appel et al., 2011; Zhang et al., 2012; Kajino and Aikawa, 2015; Qiao et al., 2015). Furthermore, gas- and particulate-phase pollutants may not come from the same source, since particulate matter can be re-emitted from natural sources and human activity. Aerosol formation is modeled separately in chemical transport models and the wet deposition of particles and gases use different parameterizations in these models. The scavenging coefficient of gases in models depends on Henry's law constant or gas diffusivity and reactivity, whereas the scavenging coefficient of particles is a function of particle size distribution and collection efficiency among other factors (Gong et al., 2011). Studies also suggest different efficiencies between rainout and washout scavenging mechanisms for gases and aerosols (Gong et al., 2011; Kajino and Aikawa, 2015). These parameterizations can differ between different chemical transport models as well leading to large uncertainties in the wet deposition estimates (Tost et al., 2007). Gas/aerosol wet scavenging observations can also be used to evaluate those from wet deposition simulations (Kajino and Aikawa, 2015).

A seasonal cycle was observed in the relative contributions of gases and particulates to nitrate, ammonium, and sulfate wet deposition. The contributions by particulates to nitrate, ammonium, and sulfate wet scavenging were greater during cold months and lower during summer (Fig. 10). This pattern is consistent with studies suggesting that particle scavenging by snow is more efficient than the scavenging by rain for an equivalent amount of precipitation (Zhang et al., 2013, 2015). Based on scavenging ratios, Zhang et al. (2015) found that snow scavenging can be 10 times more efficient than the rain scavenging of polycyclic aromatic compounds (PAC), and that snow scavenging of particulate-phase PAC can exceed that of gas-phase PAC by a similar magnitude. In contrast to particle scavenging, greater precipitation scavenging of gases was observed in the warm seasons (Fig. 10). This inverse relationship between particle and gas wet scavenging resulted because of Eq. 3, which assumes that the precipitation scavenging in excess of particle wet scavenging was due to gas scavenging. This assumption needs to be validated by independently deriving the gas scavenging contributions; however, the results based on the assumption are consistent with precipitation scavenging theories.

In terms of nitrate scavenging, the largest difference between gas and particulate wet scavenging were observed during warm months (factor of 4 higher for HNO_3), whereas smaller differences were seen during cold months (Fig. 10a). The large contribution by HNO_3 is expected because it is one of the most soluble gases and is effectively scavenged by rainout (Chang,



1984; Garrett et al., 2006). %HNO₃ were also fairly high during the cold months because of higher solubility at lower temperatures and the high absorption and retention of HNO₃ and other strong acids on ice crystals (Diehl et al., 1995; Clegg and Abbatt, 2001). Snow scavenging of HNO₃ can also exceed below-cloud rain scavenging of HNO₃ for an equivalent precipitation rate (Chang, 1984).

5 Particle wet scavenging exceeded gas scavenging contributions to ammonium wet deposition in most months by a factor of 2.6 except during May-June (Fig. 10b). For sulfate scavenging, larger differences between gas and particulate wet scavenging were found during cold months (factor of 2 higher for pSO₄⁻), while small differences were observed during warm months (Fig. 10c). The greater scavenging of pSO₄⁻ during colder months is likely attributed to the effectiveness of particle scavenging by snow as discussed earlier. Another explanation for the large disparity between particle and gas
10 scavenging in the cold months could be the low absorption of SO₂ by ice crystals especially on low pH ice surfaces (Clegg and Abbatt, 2001). As for the smaller difference between particle and gas scavenging during warm months, experiments suggest that snow scavenging of SO₂ can be increased by the presence of H₂O₂ and relatively higher temperatures of ~0°C (Mitra et al., 1990). The latter conditions are conducive to the formation of a quasi-liquid layer on the ice surface, which may increase the dissolution of SO₂ (Clegg and Abbatt, 2001).

15 4 Conclusions

Long-term air concentrations, wet deposition, and scavenging ratios of inorganic ions were analyzed using CAPMoN data. Geographical variability in the air concentrations of inorganic ions can be attributed to proximity of the sites to anthropogenic sources, oceanic sea-salt emissions, and agricultural emissions. Annual wet deposition geographical patterns for Ca²⁺, Na⁺, Cl⁻, NH₄⁺, NO₃⁻, and SO₄²⁻ were similar to those in air. Widespread declines were observed for NH₄⁺ (1994-
20 2010) and SO₄²⁻ (1983-2010) in air, which was attributed to decreases in SO₂, NO_x, and local NH₃ emissions. NO₃⁻ air concentrations increased from 1991-2001 and then decreased from 2001-2010, consistent with the trends in NO_x emissions in Canada over these two decades and in the U.S. over the last decade. However, widespread declines in annual wet deposition were only found for NO₃⁻ and SO₄²⁻ from 1984-2011. SO₄²⁻ air concentrations and annual wet deposition declined ~2 times faster in southern Ontario and southern Quebec than other locations because of the proximity of the sites to
25 industrial emission sources. Aerosol acidity and acid rain had greater impacts to southern and eastern Canada than western Canada. Temporal trends show aerosol acidity and acid rain have been decreasing simultaneously from 1994-2010, consistent with large declines in nitrate and sulfur species and slight declines or lack of change in base cations.

Scavenging ratios of particulate NH₄⁺, SO₄²⁻ and NO₃⁻ in literature may be overestimated on average by 22%, 44% and a factor of 6, respectively, because the wet scavenging of gases were excluded. The wet scavenging of HNO₃ dominated
30 particulate NO₃⁻ at most locations, while the wet scavenging of particulate NH₄⁺ and SO₄²⁻ were more efficient than NH₃ and



SO₂, respectively. The wet scavenging of particles was more efficient in the cold months likely because of the scavenging by snow. Greater gas scavenging was found in the warm months opposite in trend to particulate wet scavenging.

Long-term trends in inorganic ions provide greater insight into which Canadian regions are still susceptible to or likely recovering from acid rain impacts, and the effectiveness of environmental policies at mitigating acid rain. Particulate inorganic ions and trace gas scavenging ratios provide a measure of the wet scavenging efficiencies and are potentially useful surrogates for the wet scavenging of other pollutants provided that they have similar physicochemical properties (e.g. solubility, particle sizes, etc.). These results can be considered in future wet deposition modeling to improve the prediction of nitrate, ammonium, and sulfate wet deposition. Scavenging ratios can potentially be used to obtain a rough first order estimate of the wet deposition at other locations considering the uncertainties in both the scavenging ratios and in wet deposition modeling.

Data availability

The datasets used in this study can be accessed from the websites in the reference list or by contacting the corresponding author.

Competing interests

The authors declare that they have no conflict of interest.

Acknowledgements

The authors gratefully acknowledge the CAPMoN team of Environment and Climate Change Canada (ECCC) and the Canadian National Atmospheric Chemistry (NAtChem) Particulate Matter and Precipitation Databases and its data contributing agencies/organizations for the provision of data (1983-2011) used in this publication. The authors thank Chantale Cerny, Samantha Lee, and Bill Sukloff from ECCC for advice on climate data extraction.

References

- Appel, K. W., Foley, K. M., Bash, J. O., Pinder, R. W., Dennis, R. L., Allen D. J., and Pickering, K.: A multi-resolution assessment of the Community Multiscale Air Quality (CMAQ) model v4.7 wet deposition estimates for 2002–2006, *Geosci. Model Dev.*, 4, 357-371, doi:10.5194/gmd-4-357-2011, 2011.
- Bourcier, L., Masson, O., Laj, P., Chausse, P., Pichon, J. M., Paulat, P., Bertrand, G., and Sellegri, K.: A new method for assessing the aerosol to rain chemical composition relationships, *Atmos. Res.*, 118, 295-303, 2012.



- Cadle, S. H., VandeKopple, R., Mulawa, P. A., and Dasch, J. M.: Ambient concentrations, scavenging ratios, and source regions of acid related compounds and trace metals during winter in northern Michigan, *Atmos. Environ.*, 24(12), 2981-2989, 1990.
- Chang, T. Y.: Rain and snow scavenging of HNO₃ vapor in the atmosphere, *Atmos. Environ.* (1967), 18(1), 191-197, 1984.
- 5 Cheng, I., Zhang, L., and Mao H.: Relative contributions of gaseous oxidized mercury and fine and coarse particle-bound mercury to mercury wet deposition at nine monitoring sites in North America, *J. Geophys. Res. Atmospheres*, 120(16), 8549-8562, 2015.
- Clair, T. A., Ehrman, J. M., Ouellet, A. J., Brun, G., Lockerbie, D., and Ro, C. -U. : Changes in freshwater acidification trends in Canada's Atlantic provinces: 1983–1997, *Water Air Soil Pollut.*, 135(1-4), 335-354, 2002.
- 10 Clegg, M., and Abbatt, D.: Uptake of gas-phase SO₂ and H₂O₂ by ice surfaces: dependence on partial pressure, temperature, and surface acidity, *J. Phys. Chem. A*, 105(27), 6630-6636, 2001.
- Cole, A. S., Steffen, A., Eckley, C. S., Narayan, J., Pilote, M., Tordon, R., Graydon, J. A., St. Louis, V. L., Xu, X., and Branfireun, B. A.: A survey of mercury in air and precipitation across Canada: patterns and trends, *Atmosphere*, 5(3), 635-668, 2014.
- 15 Dana, M. T.: SO₂ versus sulfate wet deposition in the eastern United States, *J. Geophys. Res. Oceans*, 85(C8), 4475-4480, 1980.
- Diehl, K., Mitra, S. K., and Pruppacher, H. R.: A laboratory study of the uptake of HNO₃ and HCl vapor by snow crystals and ice spheres at temperatures between 0 and – 40 C, *Atmos. Environ.*, 29(9), 975-981, 1995.
- Driscoll, C. T., Lawrence, G. B., Bulger, A. J., Butler, T. J., Cronan, C. S., Eagar, C., Lambert, K. F., Likens, G. E.,
- 20 Stoddard, J. L., and Weathers, K. C.: Acidic Deposition in the Northeastern United States: Sources and Inputs, Ecosystem Effects, and Management Strategies, *Bioscience*, 51(3), 180-198, 2001.
- Driscoll, C. T., Driscoll, K. M., Roy, K. M., and Mitchell, M. J.: Chemical response of lakes in the Adirondack region of New York to declines in acidic deposition, *Environ. Sci. Technol.*, 37(10), 2036-2042, 2003.
- Duce, R. A., Liss, P. S., Merrill, J. T., Atlas, E. L., Buat-Menard, P., Hicks, B. B., Miller, J.M., Prospero, J. M., Arimoto, R.,
- 25 Church, J. M., Ellis, W., Galloway, J. N., Hansen, L., Jickells, T. D., Knap, A. H., Reinhardt, K. H., Schneider, B., Soudine, A., Tokos, J. J., Tsunogai, S., Wollast, R., and Zhou, M.: The atmospheric input of trace species to the world ocean, *Global Biogeochem. Cycles*, 5, 193-259, 1991.
- Encinas, D., Calzada, I., and Casado, H.: Scavenging ratios in an urban area in the Spanish Basque country, *Aerosol Sci. Technol.*, 38(7), 685-691, 2004.
- 30 Environment Canada: National Pollutant Release Inventory (NPRI), Air pollutant emission inventory – online data search, Emission trends, available at: <http://www.ec.gc.ca/inrp-npri/donnees-data/ap/index.cfm?lang=En>, 2014 (Accessed 15 December 2015)



- Environment Canada: Canadian National Atmospheric Chemistry (NAtChem) Particulate Matter and Precipitation Chemistry Database. Science and Technology Branch, 4905 Dufferin Street, Toronto, Ontario, Canada M3H 5T4. Available at: <http://www.on.ec.gc.ca/natchem/Login/Login.aspx>, 2015a (Accessed 1 October 2015)
- Environment Canada: Canadian Climate Data Archives, Ontario Climate Center, Meteorological Service of Canada, 4905
5 Dufferin Street, Toronto, Ontario, Canada M3H 5T4, 2015b.
- Fischer, E., Pszenny, A., Keene, W., Maben, J., Smith, A., Stohl, A., and Talbot, R.: Nitric acid phase partitioning and cycling in the New England coastal atmosphere, *J. Geophys. Res. Atmospheres*, 111, D23S09, doi:[10.1029/2006JD007328](https://doi.org/10.1029/2006JD007328), 2006.
- Galloway, J. N., Savoie, D. L., Keene, W. C., and Prospero, J. M.: The temporal and spatial variability of scavenging ratios
10 for NSS sulfate, nitrate, methanesulfonate and sodium in the atmosphere over the North Atlantic Ocean, *Atmos. Environ.*, 27(2), 235-250, 1993.
- Garrett, T. J., Avey, L., Palmer, P. I., Stohl, A., J. Neuman, A., Brock, C. A., Ryerson, T. B., Holloway, J. S.: Quantifying wet scavenging processes in aircraft observations of nitric acid and cloud condensation nuclei, *J. Geophys. Res. Atmospheres*, 111, D23S51, doi:[10.1029/2006JD007416](https://doi.org/10.1029/2006JD007416), 2006.
- 15 Gilbert, R. O.: *Statistical Methods for Environmental Pollution Monitoring*, Van Nostrand Reinhold Company Inc., New York, USA, 1987.
- Gong, W., Stroud, C., and Zhang, L.: Cloud processing of gases and aerosols in air quality modeling, *Atmosphere*, 2(4), 567-616, 2011.
- Granat, L., Engström, J. E., Praveen, S., and Rodhe, H.: Light absorbing material (soot) in rainwater and in aerosol particles
20 in the Maldives, *J. Geophys. Res. Atmospheres*, 115(D16307), doi:[10.1029/2009JD013768](https://doi.org/10.1029/2009JD013768), 2010.
- Guerzoni, S., Cristini, A., Caboi, R., Le Bolloch, O., Marras, I., and Rundeddu, L.: Ionic composition of rainwater and atmospheric aerosols in Sardinia, southern Mediterranean, *Water Air Soil Pollut.*, 85(4), 2077-2082, 1995.
- Hales, J. M. and Dana, M. T.: Regional-scale deposition of sulfur dioxide by precipitation scavenging, *Atmos. Environ.*, 13(8), 1121-1132, 1979.
- 25 Hames, R. S., Rosenberg, K. V., Lowe, J. D., Barker, S. E., and Dhondt, A. A.: Adverse effects of acid rain on the distribution of the Wood Thrush *Hylocichla mustelina* in North America, *Proc. Natl. Acad. Sci.*, 99(17), 11235-11240, 2002.
- He, J., and Balasubramanian, R.: Rain-aerosol coupling in the tropical atmosphere of Southeast Asia: distribution and scavenging ratios of major ionic species, *J. Atmos. Chem.*, 60(3), 205-220, 2008.
- He, K., Zhao, Q., Ma, Y., Duan, F., Yang, F., Shi, Z., and Chen, G.: Spatial and seasonal variability of PM 2.5 acidity at two
30 Chinese megacities: insights into the formation of secondary inorganic aerosols, *Atmos. Chem. Phys.*, 12(3), 1377-1395, 2012.
- Hedin, L. O., Granat, L., Likens, G. E., Adri Buishand, T., Galloway, J. N., Butler, T. J., and Rodhe, H.: Steep declines in atmospheric base cations in regions of Europe and North America, *Nature*, 367, 351-354, 1994.



- Hennigan, C. J., Bergin, M. H., Dibb, J. E., and Weber, R. J.: Enhanced secondary organic aerosol formation due to water uptake by fine particles, *Geophys. Res. Lett.*, 35(18), L18801, doi:[10.1029/2008GL035046](https://doi.org/10.1029/2008GL035046), 2008.
- Hennigan, C. J., Izumi, J., Sullivan, A. P., Weber, R. J., and Nenes, A.: A critical evaluation of proxy methods used to estimate the acidity of atmospheric particles, *Atmos. Chem. Phys.*, 15(5), 2775-2790, 2015.
- 5 Hicks, B. B.: A climatology of wet deposition scavenging ratios for the United States, *Atmos. Environ.*, 39(9), 1585-1596, 2005.
- Jeffries, D. S., Brydges, T. G., Dillon, P. J., and Keller, W.: Monitoring the results of Canada/USA acid rain control programs: some lake responses, *Environ. Monit. Assess.*, 88(1-3), 3-19, 2003.
- Kajino, M. and Aikawa, M.: A model validation study of the washout/rainout contribution of sulfate and nitrate in wet
10 deposition compared with precipitation chemistry data in Japan, *Atmos. Environ.*, 117, 124-134, 2015.
- Kasper-Giebl, A., Kalina, M. F., and Puxbaum, H.: Scavenging ratios for sulfate, ammonium and nitrate determined at Mt. Sonnblick (3106 m.a.s.l.), *Atmos. Environ.*, 33(6), 895-906, 1999.
- Kerminen, V. M., Hillamo, R., Teinilä, K., Pakkanen, T., Allegrini, I., and Sparapani, R.: Ion balances of size-resolved tropospheric aerosol samples: implications for the acidity and atmospheric processing of aerosols, *Atmos. Environ.*, 35(31),
15 5255-5265, 2001.
- Kothawala, D. N., Watmough, S. A., Futter, M. N., Zhang, L., and Dillon, P. J.: Stream nitrate responds rapidly to decreasing nitrate deposition. *Ecosystems*, 14, 274-286, 2011.
- Kulshrestha, U. C., Reddy, L. A. K., Satyanarayana, J., and Kulshrestha, M. J.: Real-time wet scavenging of major chemical constituents of aerosols and role of rain intensity in Indian region, *Atmos. Environ.*, 43(32), 5123-5127, 2009.
- 20 Lawrence, G. B., Hazlett, P. W., Fernandez, I. J., Ouimet, R., Bailey, S. W., Shortle, W. C., Smith, K. T., and Antidormi, M. R.: Declining Acidic Deposition Begins Reversal of Forest-Soil Acidification in the Northeastern US and Eastern Canada, *Environ. Sci. Technol.*, 49(22), 13103-13111, 2015.
- Lehmann, C. M., Bowersox, V. C., and Larson S. M.: Spatial and temporal trends of precipitation chemistry in the United States, 1985–2002, *Environ. Pollut.*, 135(3), 347-361, 2005.
- 25 Lehmann, C. M., Bowersox, V. C., Larson, R. S., and Larson, S. M.: Monitoring long-term trends in sulfate and ammonium in US precipitation: Results from the National Atmospheric Deposition Program/National Trends Network, *Water Air Soil Pollut.*, 7, 59-66, 2007.
- Lloret, J. and Valiela, I.: Unprecedented decrease in deposition of nitrogen oxides over North America: the relative effects of emission controls and prevailing air-mass trajectories, *Biogeochem.*, doi:10.1007/s10533-016-0225-5, 2016.
- 30 McMillan, A. C., MacIver, D., and Sukloff, W. B.: Atmospheric environmental information—an overview with Canadian examples, *Environ. Modell. Softw.*, 15(3), 245-248, 2000.
- Mitra, S. K., Barth, S. and Pruppacher, H. R.: A laboratory study on the scavenging of SO₂ by snow crystals, *Atmos. Environ.*, 24(9), 2307-2312, 1990.



- Ontario Ministry of Energy (MOE): The End of Coal, available at: <http://www.energy.gov.on.ca/en/archive/the-end-of-coal/>, 2015 (Accessed 3 February 2016)
- Pitchford, M. L., Poirot, R. L., Schichtel, B. A., and Maim, W. C.: Characterization of the winter midwestern particulate nitrate bulge, *J. Air Waste Manag. Assoc.*, 58(9), 1061–9, 2009.
- 5 Prestbo, E. M. and Gay, D. A.: Wet deposition of mercury in the US and Canada, 1996–2005: Results and analysis of the NADP mercury deposition network (MDN), *Atmos. Environ.*, 43(27), 4223–4233, 2009.
- Pryor, S. C. and Sørensen, L. L.: Nitric acid-sea salt reactions: Implications for nitrogen deposition to water surfaces, *J. Appl. Meteorol.*, 39(5), 725–731, 2000.
- Qiao, X., Tang, Y., Hu, J., Zhang, S., Li, J., Kota, S. H., Wu, L., Gao, H., Zhang, H., and Ying, Q.: Modeling dry and wet
10 deposition of sulfate, nitrate, and ammonium ions in Jiuzhaigou National Nature Reserve, China using a source-oriented CMAQ model: Part I. Base case model results, *Sci. Total Environ.*, 532, 831–839, 2015.
- Sakata, M., and Asakura, K.: Estimating contribution of precipitation scavenging of atmospheric particulate mercury to mercury wet deposition in Japan, *Atmos. Environ.*, 41(8), 1669–1680, 2007.
- Sander, R.: Compilation of Henry's law constants (version 4.0) for water as solvent, *Atmos. Chem. Phys.*, 15(8), 4399–4981,
15 2015.
- Shrestha, A. B., Wake, C. P., Dibb, J. E., and Whitlow, S. I.: Aerosol and precipitation chemistry at a remote Himalayan site in Nepal, *Aerosol Sci. Technol.*, 36(4), 441–456, 2002.
- Stoddard, J. L., Jeffries, D. S., Lükewille, A., Clair, T. A., Dillon, P. J., Driscoll, C. T., Forsius, M., Johannessen, M., Kahl, J. S., Kellogg, J. H., and Kemp, A.: Regional trends in aquatic recovery from acidification in North America and Europe,
20 *Nature*, 401(6753), 575–578, 1999.
- Strock, K. E., Nelson, S. J., Kahl, J. S., Saros, J. E., and McDowell, W. H.: Decadal trends reveal recent acceleration in the rate of recovery from acidification in the northeastern US, *Environ. Sci. Technol.*, 48(9), 4681–4689, 2014.
- Tost, H., Jöckel, P., Kerkweg, A., Pozzer, A., Sander, R., and Lelieveld J.: Global cloud and precipitation chemistry and wet deposition: tropospheric model simulations with ECHAM5/MESy1, *Atmos. Chem. Phys.*, 7(10), 2733–2757, 2007.
- 25 Tuncel, S. G. and Ungör, S.: Rain water chemistry in Ankara, Turkey, *Atmos. Environ.*, 30(15), 2721–2727, 1996.
- USEPA: 2011 National Emissions Inventory Data, available at: <http://www3.epa.gov/ttnchie1/net/2011inventory.html>, 2015 (Accessed 15 December 2015)
- Vogt, R. D., Seip, H. M., Larssen, T., Zhao, D., Xiang, R., Xiao, J., Luo, J., and Zhao, Y.: Potential acidifying capacity of deposition: Experiences from regions with high NH₄⁺ and dry deposition in China, *Sci. Total Environ.*, 367(1), 394–404,
30 2006.
- Wang, X., Zhang, L., and Moran, M. D.: Bulk or modal parameterizations for below-cloud scavenging of fine, coarse, and giant particles by both rain and snow, *J. Adv. Model Earth Sy.*, 6(4), 1301–1310, 2014.
- Watmough, S. A. and Dillon, P. J.: Base cation and nitrogen budgets for a mixed hardwood catchment in south-central Ontario, *Ecosystems*, 6(7), 675–693, 2003.



- Watmough, S. A., Aherne, J., Alewell, C., Arp, P., Bailey, S., Clair, T., Dillon, P., Duchesne, L., Eimers, C., Fernandez, I., and Foster, N.: Sulphate, nitrogen and base cation budgets at 21 forested catchments in Canada, the United States and Europe, *Environ. Monit. Assess.*, 109(1-3), 1-36, 2005.
- Yao, X., Chan, C. K., Fang, M., Cadle, S., Chan, T., Mulawa, P., He, K., and Ye, B.: The water-soluble ionic composition of PM_{2.5} in Shanghai and Beijing, China, *Atmos. Environ.*, 36(26), 4223-4234, 2002.
- Zbieranowski, A. L. and Aherne, J.: Long-term trends in atmospheric reactive nitrogen across Canada: 1988–2007, *Atmos. Environ.*, 45(32), 5853-5862, 2011.
- Zhang, L., Vet, R. and Michelangeli, D. V.: Numerical investigation of gas scavenging by weak precipitation, *J. Atmos. Chem.*, 54(3), 203-231, 2006.
- 10 Zhang, L., Jacob, D. J., Knipping, E. M., Kumar, N., Munger, J. W., Carouge, C. C., van Donkelaar, A., Wang, Y. X., and Chen, D.: Nitrogen deposition to the United States: distribution, sources, and processes, *Atmos. Chem. Phys.*, 12, 4539-4554, doi:10.5194/acp-12-4539-2012, 2012.
- Zhang, L., Vet, R., Wiebe, A., Mihele, C., Sukloff, B., Chan, E., Moran, M. D., and Iqbal, S.: Characterization of the size segregated water-soluble inorganic ions at eight Canadian rural sites. *Atmos. Chem. Phys.*, 8, 7133–7151, doi:10.5194/acp-15 8-7133-2008, 2008.
- Zhang, L., Wang, X., Moran, M. D., and Feng, J.: Review and uncertainty assessment of size-resolved scavenging coefficient formulations for below-cloud snow scavenging of atmospheric aerosols, *Atmos. Chem. Phys.*, 13, 10005–10025, doi:10.5194/acp-13-10005-2013, 2013.
- Zhang, L., Cheng, I., Muir, D., and Charland, J. -P.: Scavenging ratios of polycyclic aromatic compounds in rain and snow at the Athabasca oil sands region, *Atmos. Chem. Phys.*, 15, 1421–1434, 2015.
- Zhang, Q., Jimenez, J. L., Worsnop, D. R., and Canagaratna, M.: A case study of urban particle acidity and its influence on secondary organic aerosol, *Environ. Sci. Technol.*, 41(9), 3213-3219, 2007.
- Zhao, Y. and Gao, Y.: Mass size distributions of water-soluble inorganic and organic ions in size-segregated aerosols over metropolitan Newark in the US east coast, *Atmos. Environ.*, 42(18), 4063-4078, 2008.
- 25 Ziemba, L. D., Fischer, E., Griffin, R. J., and Talbot, R. W.: Aerosol acidity in rural New England: Temporal trends and source region analysis, *J. Geophys. Res. Atmos.*, 112(D10S22), doi:10.1029/2006JD007605, 2007.



Table 1: Site and data descriptions. NA indicates no available data. Short-term data were not analyzed. Refer to Fig. S1 for a map of the sites.

Site name	Province	Latitude	Longitude	Elevation (m)	Coastal/inland	Land use	Air data	Wet deposition data
Saturna	BC	48.78	-123.13	178	Coastal	Forest	Dec 1990-Dec 2010	Jan 1990-Dec 2011
Snare Rapids	NT	63.52	-116.00	240	Inland	Forest	NA	Jan 1989-Dec 2011
Esther	AB	51.67	-110.20	707	Inland	Agricultural	Oct 1991-Mar 2003	Jan 1987-Dec 2002, Jan 2009-Dec 2011
Cree Lake	SK	57.35	-107.13	499	Inland	Forest	Jul 1982-May 1993	Jan 1984-Dec 1992
Bratt's Lake	SK	50.20	-104.71	600	Inland	NA	Aug 2001-Dec 2010	Jan 2001-Dec 2011
McCreary	MB	50.71	-99.53	335	Inland	Agricultural	NA	Jan 1984-Dec 1995
Island Lake	MB	53.87	-94.67	245	Inland	Forest	NA	Jan 1984-Dec 1997
Experimental Lakes Area (ELA)	ON	49.66	-93.72	369	Inland	Forest	Jan 1979-Dec 2010	Jan 1984-Dec 2011
Pickle Lake B	ON	51.45	-90.22	370	Inland	Forest	NA	Jan 2003-Dec 2011
Algoma	ON	47.04	-84.38	411	Inland	Forest	Oct 1980-Dec 2010	Jan 1985-Dec 2011
Burnt Island	ON	45.82	-82.95	185	Inland	Forest	NA	Jan 1992-Dec 2011
Bonner Lake	ON	49.39	-82.12	245	Inland	Forest	short-term	Jun 1985-Dec 2011
Longwoods	ON	42.88	-81.48	239	Inland	Agricultural	Jan 1983-Dec 2010	Jan 1984-Dec 2011
Priceville	ON	44.17	-80.66	475	Inland	Agricultural	NA	Jan 1985-Dec 1994
Egbert	ON	44.23	-79.78	253	Inland	Agricultural	Jul 1988-Dec 2010	Jan 1989-Dec 2011
Egbert-2	ON	44.23	-79.78	253	Inland	Agricultural	short-term	Jan 1997-Dec 2011
Sprucedale	ON	45.42	-79.49	350	Inland	Agricultural	May 2002-Dec 2010	Jan 2003-Dec 2011
Warsaw Caves	ON	44.46	-78.13	230	Inland	Agricultural	NA	Jan 1986-Dec 2011
Chalk River	ON	46.06	-77.41	184	Inland	Forest	Jan 1979-Dec 2010	Jan 1984-Dec 2011
Chapais	QC	49.82	-74.98	381	Inland	Forest	Jun 1988-Dec 2010	Jan 1988-Dec 2011
Frelighsburg	QC	45.05	-72.86	203	Inland	Agricultural	Nov 2001-Dec 2010	Jan 2002-Dec 2011
Sutton	QC	45.08	-72.68	243	Inland	Forest	Jan 1986-Mar 2002	Jan 1984-Dec 2001
Lac Edouard	QC	47.68	-72.44	243	Inland	Forest	Jan 2002-Dec 2010	Jan 2002-Dec 2011
Montmorency	QC	47.32	-71.15	640	Coastal	Forest	Dec 1980-Jan 1997	Jan 1984-Dec 1996
Harcourt	NB	46.50	-65.27	37	Coastal	Forest	NA	Jan 1984-Dec 2011
Kejimikujik	NS	44.43	-65.21	127	Coastal	Forest	May 1979-Dec 2010	Jan 1984-Dec 2011
Mingan	QC	50.27	-64.22	14	Coastal	Forest	short-term	Jan 1994-Dec 2011
Jackson	NS	45.59	-63.84	90	Coastal	Forest	NA	Jan 1984-Dec 2011
Goose Bay	NL	53.31	-60.36	39	Coastal	Forest	NA	Jan 1984-Dec 2011
Goose Bay B	NL	53.29	-60.39	39	Coastal	Forest	NA	Jan 1989-Dec 2007
Bay d'Espoir	NL	47.99	-55.81	190	Coastal	Forest	short-term	Jan 1984-Dec 2011



Table 2: Rate of change in annual air concentrations. Slope refers to the Seasonal Kendall slope ($\text{ng m}^{-3} \text{a}^{-1}$); C.I. refers to the 90% confidence interval of the slope; ns indicates no significant trend; na indicates no available data.

Site	Ca^{2+}		Mg^{2+}		K^+		Na^+		Cl^-	
	Slope	C.I.	Slope	C.I.	Slope	C.I.	Slope	C.I.	Slope	C.I.
Saturna	-0.9	-1.3 to -0.6	-0.8	-1.1 to -0.4	-0.7	-1 to -0.5	-4.5	-6.5 to -1.8	1.0	ns
Esther	9.9	4.8 to 15.8	1.5	0.9 to 2.5	1.3	0.8 to 1.8	2.1	0.8 to 3.6	-0.4	-0.7 to 0
Cree Lake	na	na	na	na	-1.3	-2 to -0.5	0.5	ns	-0.5	-1 to -0.1
Bratt's Lake	5.5	ns	2.4	ns	-3.8	-5.3 to -2.4	-2.4	-4.2 to -1.3	-0.6	-1.3 to -0.2
ELA	0.5	ns	-0.2	ns	-0.5	-0.6 to -0.3	-0.7	-0.8 to -0.5	-0.2	-0.4 to -0.2
Algoma	-0.3	ns	-0.2	-0.5 to 0	-0.6	-0.8 to -0.5	-0.3	-0.5 to -0.2	-0.1	-0.2 to 0
Longwoods	-15.9	-21.1 to -10	-1.1	-2.1 to -0.4	-0.6	-0.9 to -0.3	-0.5	-0.8 to -0.2	-0.8	-1 to -0.5
Egbert	-9.7	-14.8 to -3.6	0.1	ns	0.02	ns	-0.2	ns	0.2	ns
Sprucedale	-2.7	ns	-0.9	ns	-1.2	-1.8 to -0.6	-1.3	-1.9 to -0.4	-0.2	ns
Chalk River	-0.3	ns	-0.6	-0.8 to -0.4	-0.8	-1 to -0.6	-0.5	-0.8 to -0.3	0.03	ns
Chapais	0.4	ns	-0.03	ns	-0.5	-0.6 to -0.4	-0.9	-1.2 to -0.7	0.3	0 to 0.6
Frelighsburg	-0.8	ns	0.3	ns	-1.1	-1.8 to -0.7	-2.6	-4.4 to -0.7	-0.01	ns
Sutton	1.5	ns	0.2	ns	-1.8	-2.3 to -1.4	-1.8	-2.3 to -1.4	-0.2	ns
Lac Edouard	-0.01	ns	-0.2	ns	-1.0	-1.4 to -0.6	-1.4	-2.1 to -0.5	-0.4	ns
Montmorency	na	na	na	na	-0.6	-1.1 to 0	1.4	0.8 to 2.1	0.1	ns
Kejimkujik	0.4	0 to 0.8	-0.5	-0.8 to -0.1	-0.5	-0.7 to -0.4	1.8	0.4 to 3	4.9	3.7 to 6.6

Site	NH_4^+		NO_3^-		SO_4^{2-}		SO_2		HNO_3	
	Slope	C.I.	Slope	C.I.	Slope	C.I.	Slope	C.I.	Slope	C.I.
Saturna	-7.6	-9.1 to -6.2	-9.3	-12.8 to -5.6	-28.8	-32.6 to -25.2	-62.6	-72.5 to -52.5	-17.1	-20.7 to -13.6
Esther	7.9	2 to 15.6	40.1	32.6 to 50.4	7.0	ns	-6.5	ns	12.0	2.2 to 21.8
Cree Lake	3.7	1.1 to 6.2	-1.1	ns	0.0	ns	8.4	ns	8.9	6 to 11.4
Bratt's Lake	-16.5	-23.4 to -9.7	-21.4	-34.3 to -10.5	-30.4	-51.1 to -11.8	1.6	ns	-19.4	-27.3 to -13.3
ELA	-4.4	-6 to -2.6	3.5	1.7 to 5.2	-28.4	-32.1 to -24.4	-14.6	-17.7 to -12.2	-2.3	-3.7 to -0.8
Algoma	-7.0	-9.9 to -3.7	6.4	4.4 to 8.4	-46.8	-55 to -39	-77.4	-87.2 to -67.3	-3.8	-7.1 to -0.9
Longwoods	-28.8	-34.4 to -23.1	-15.2	-22.9 to -6.5	-97.4	-110.2 to -87.4	-221.5	-240.2 to -202.1	-27.6	-32.7 to -23.3
Egbert	-41.8	-49.3 to -35.5	-34.2	-43.2 to -23.6	-93.9	-108.9 to -81.5	-199.4	-221.6 to -177.3	-25.1	-31.2 to -19.5
Sprucedale	-32.8	-52.4 to -12.6	-29.5	-39.9 to -16.6	-99.0	-150.5 to -36.8	-140.0	-188.7 to -97.2	-54.4	-74.5 to -36.3
Chalk River	-8.8	-11.6 to -6.4	2.8	1.5 to 4.3	-59.8	-66.9 to -52.1	-104.7	-115.3 to -94.1	-8.2	-10.8 to -5.7
Chapais	-5.7	-7 to -4.2	1.3	0.8 to 2	-41.3	-46.3 to -36	-45.5	-52.3 to -39.6	-4.3	-5.8 to -3.1
Frelighsburg	-58.2	-69 to -45.4	-53.4	-68.6 to -38.9	-108.6	-139.5 to -84	-160.8	-206 to -119.7	-81.7	-91.2 to -68.9
Sutton	-4.6	ns	18.8	13.9 to 24.2	-64.2	-80.4 to -51.2	-90.1	-112.8 to -67.3	-12.7	-18.9 to -4
Lac Edouard	-20.3	-27.9 to -13.1	-11.0	-14.3 to -6.4	-64.8	-88 to -47.6	-55.8	-76.2 to -34.1	-35.9	-42.4 to -27.1
Montmorency	9.6	6.1 to 14.6	5.9	4.5 to 8.2	-1.0	ns	-20.1	-40 to -3.2	21.0	14.9 to 29
Kejimkujik	-5.3	-6.5 to -4	2.5	1.4 to 3.8	-53.1	-59 to -47.5	-35.9	-41.2 to -30	-6.5	-7.9 to -4.8



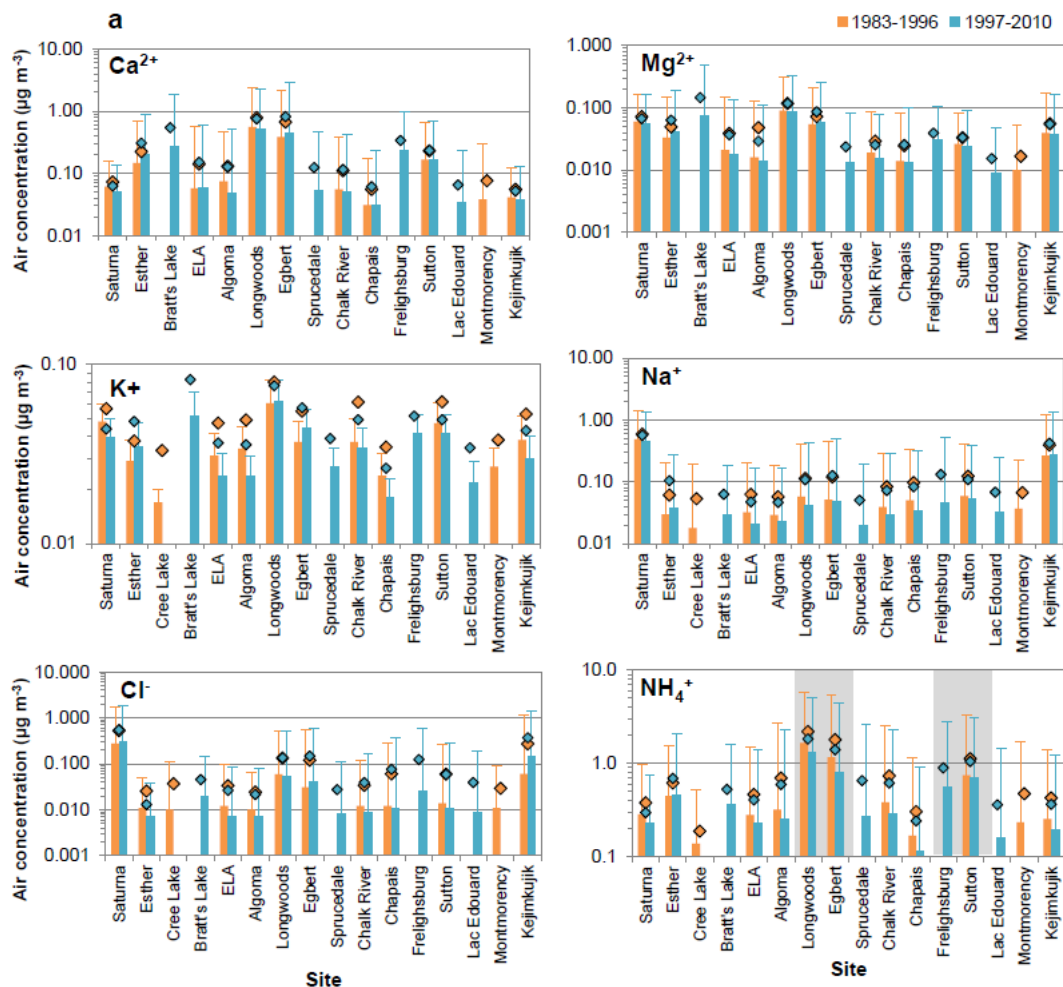
Table 3: Rate of change in annual wet deposition of Ca^{2+} , Mg^{2+} , K^+ , Na^+ , and Cl^- . Slope refers to the Sen's slope ($\text{kg ha}^{-1} \text{ a}^{-1}$); C.I. refers to the 90% confidence interval of the slope; ns indicates no significant trend.

Site	Ca^{2+}		Mg^{2+}		K^+		Na^+		Cl^-	
	Slope	C.I.	Slope	C.I.	Slope	C.I.	Slope	C.I.	Slope	C.I.
Saturna	0.001	ns	-0.0003	ns	-0.0002	ns	0.001	ns	0.002	ns
Esther	0.010	ns	0.003	ns	0.002	ns	0.002	ns	-0.001	ns
Cree Lake	-0.014	ns	-0.001	ns	-0.003	ns	0.001	ns	-0.002	ns
Bratt's Lake	0.036	ns	0.009	ns	0.005	ns	0.002	ns	0.001	ns
ELA	0.008	ns	0.002	ns	0.002	ns	-0.002	-0.004 to -0.0002	-0.001	ns
Algoma	-0.009	ns	-0.003	-0.0064 to -0.0005	-0.003	-0.0059 to -0.0003	-0.004	ns	-0.015	-0.025 to -0.01
Longwoods	-0.017	ns	-0.002	ns	0.006	0.003 to 0.011	0.004	ns	-0.013	-0.023 to -0.003
Egbert	0.003	ns	-0.001	ns	-0.0005	ns	0.004	0.002 to 0.009	-0.008	ns
Sprucedale	-0.024	ns	-0.008	-0.015 to -0.003	-0.002	ns	-0.005	ns	-0.037	ns
Chalk River	0.001	ns	-0.001	ns	-0.001	ns	0.001	ns	-0.008	-0.013 to -0.004
Chapais	0.004	ns	-0.001	-0.0022 to -0.0003	-0.0002	ns	-0.003	-0.006 to -0.001	-0.007	-0.012 to -0.002
Frelighsburg	0.020	ns	0.001	ns	0.001	ns	0.002	ns	-0.012	ns
Sutton	-0.029	-0.058 to -0.005	-0.002	ns	-0.001	ns	0.002	ns	-0.006	ns
Lac Edouard	-0.004	ns	-0.002	ns	-0.002	ns	-0.014	-0.022 to -0.001	-0.025	-0.046 to -0.008
Montmorency	-0.023	ns	-0.002	ns	0.001	ns	0.009	0.0009 to 0.016	0.006	ns
Kejimikujik	0.007	ns	0.003	ns	-0.0003	ns	0.024	ns	0.056	ns



Table 4: Rate of change in annual wet deposition of NH_4^+ , NO_3^- , SO_4^{2-} , nss- SO_4^{2-} , precipitation amount and pH. Slope refers to the Sen's slope ($\text{kg ha}^{-1} \text{a}^{-1}$); C.I. refers to the 90% confidence interval of the slope; ns indicates no significant trend; na indicates no available data.

Site	NH_4^+		NO_3^-		SO_4^{2-}		nss- SO_4^{2-}		Annual precip (mm a^{-1})		pH (a^{-1})	
	Slope	C.I.	Slope	C.I.	Slope	C.I.	Slope	C.I.	Slope	C.I.	Slope	C.I.
Saturna	-0.01	ns	-0.07	-0.13 to -0.01	-0.13	-0.17 to -0.06	-0.12	-0.16 to -0.07	-1.5	ns	0.012	0.009 to 0.016
Esther	0.02	ns	0.04	ns	-0.02	ns	na	na	-1.4	ns	-0.012	ns
Cree Lake	-0.02	ns	-0.05	ns	-0.09	ns	na	na	-2.0	ns	-0.010	ns
Bratt's Lake	0.07	ns	0.02	ns	0.10	ns	na	na	25.9	ns	-0.009	ns
ELA	0.05	0.03 to 0.07	0.02	ns	-0.04	ns	na	na	6.0	ns	0.009	0.003 to 0.014
Algoma	-0.06	-0.09 to -0.02	-0.38	-0.51 to -0.26	-0.60	-0.71 to -0.47	na	na	-7.8	-14.5 to -2.7	0.020	0.016 to 0.025
Longwoods	0.03	ns	-0.33	-0.48 to -0.17	-0.55	-0.7 to -0.36	na	na	3.9	ns	0.023	0.019 to 0.028
Egbert	-0.001	ns	-0.31	-0.45 to -0.18	-0.45	-0.57 to -0.33	na	na	3.8	ns	0.027	0.022 to 0.03
Sprucedale	-0.03	ns	-1.01	-1.4 to -0.48	-1.00	-1.46 to -0.36	na	na	9.1	ns	0.030	0.018 to 0.042
Chalk River	0.01	ns	-0.19	-0.24 to -0.11	-0.36	-0.43 to -0.29	na	na	5.3	2.1 to 8.3	0.020	0.018 to 0.022
Chapais	-0.01	ns	-0.21	-0.28 to -0.11	-0.34	-0.45 to -0.25	na	na	-0.9	ns	0.015	0.013 to 0.018
Frelighsburg	-0.02	ns	-0.93	-1.29 to -0.64	-0.93	-1.57 to -0.16	na	na	13.5	ns	0.056	0.036 to 0.069
Sutton	0.05	0.01 to 0.09	0.01	ns	-0.57	-0.9 to -0.23	na	na	4.0	ns	0.017	0.01 to 0.026
Lac Edouard	-0.07	ns	-0.69	-0.91 to -0.38	-0.46	-0.77 to -0.23	na	na	14.6	ns	0.027	0.018 to 0.045
Montmorency	0.05	ns	0.20	ns	-0.27	ns	-0.27	ns	27.8	6.1 to 45.7	0.008	0.001 to 0.014
Kejimikujik	0.01	ns	-0.12	-0.18 to -0.06	-0.27	-0.37 to -0.2	-0.28	-0.36 to -0.2	10.9	3 to 17.2	0.014	0.011 to 0.017



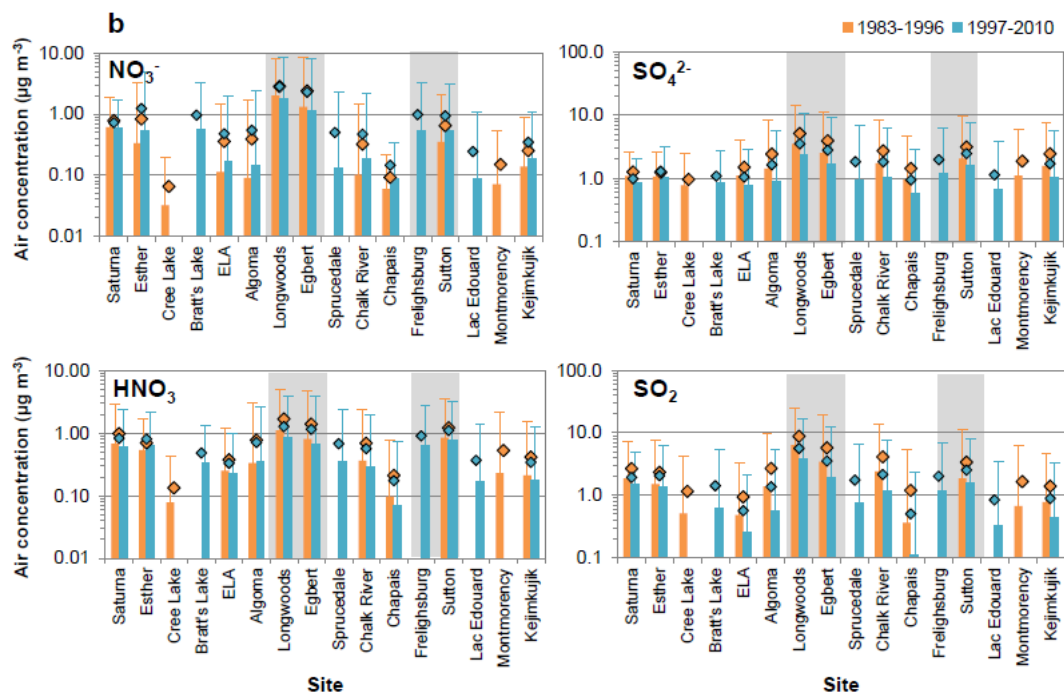


Figure 1: Geographical patterns of base cations, Cl^- and NH_4^+ (a) and NO_3^- , SO_4^{2-} , HNO_3 and SO_2 (b) for the 1983-1996 and 1997-2010 periods. Sites are arranged in order from western to eastern Canada. Bars indicate the median concentration. Error bars indicate the 95th percentile concentration. Diamonds indicate the mean concentration. Grey shaded regions correspond to southern Ontario or southern Quebec sites.

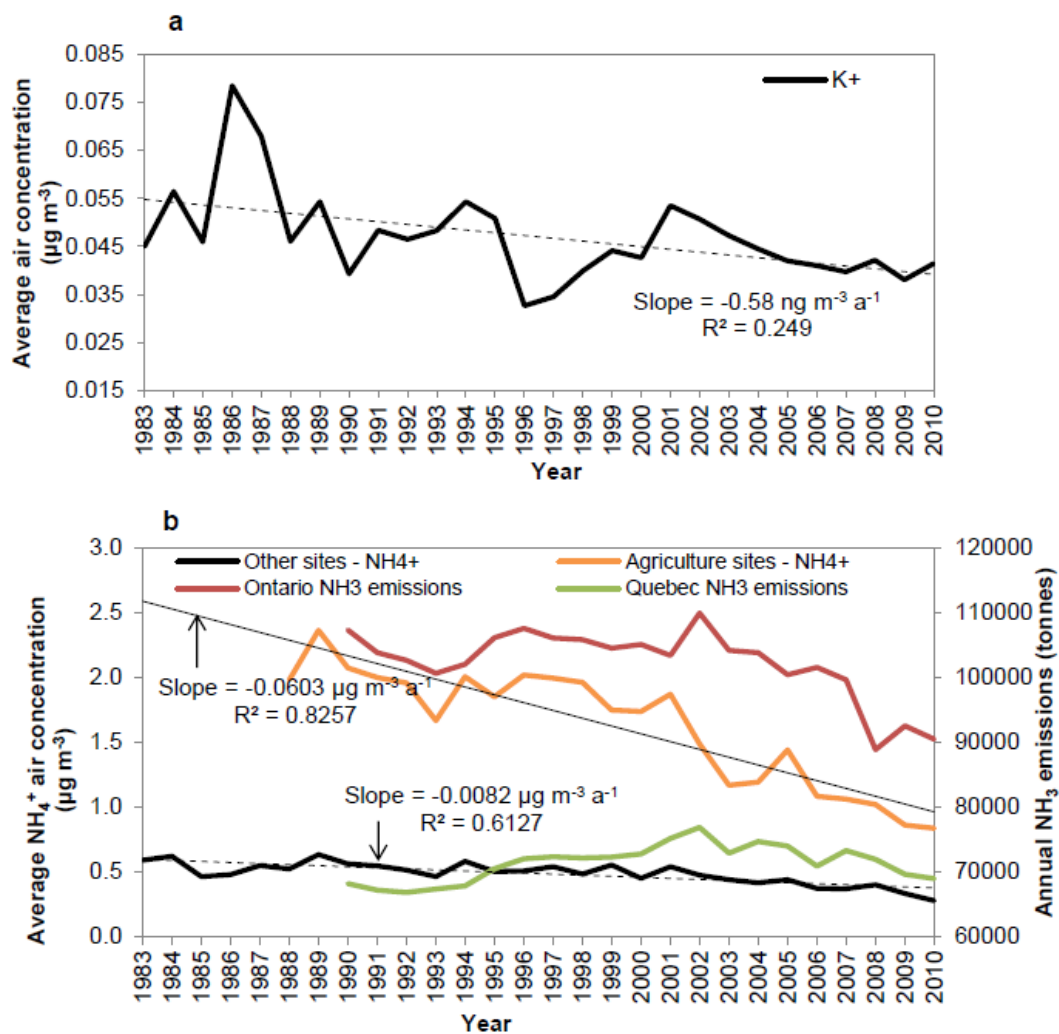


Figure 2: Temporal trends of annual average atmospheric K^+ (a) and atmospheric NH_4^+ and annual ammonia emissions (b).

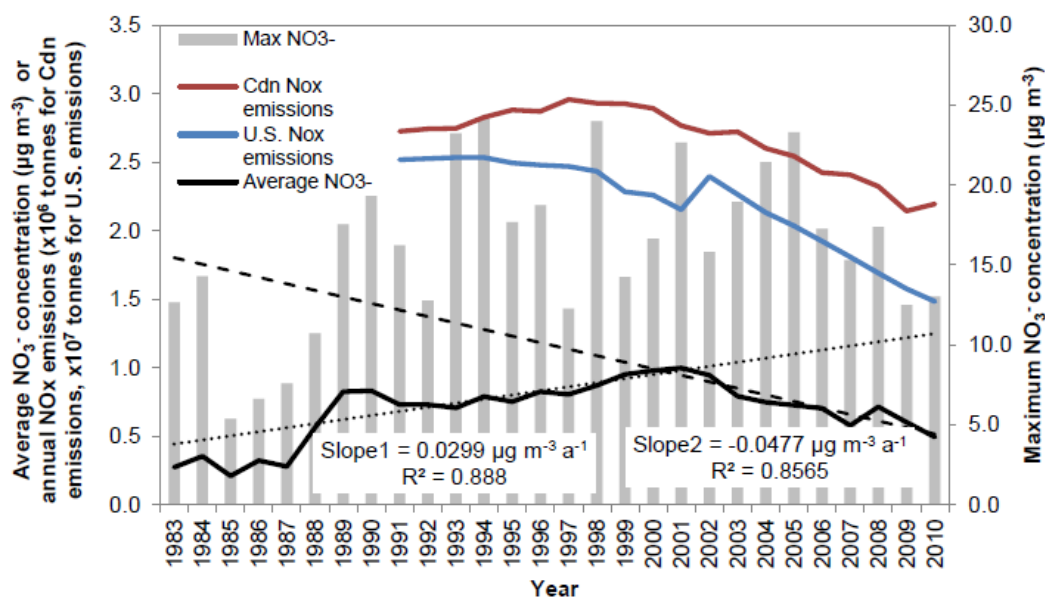


Figure 3: Temporal trends of annual atmospheric NO₃⁻ and annual NO_x emissions. Slope1 refers to the regression line for NO₃⁻ between 1991 and 2001 (positive trend), while Slope2 is for the period between 2001 and 2010 (negative trend).

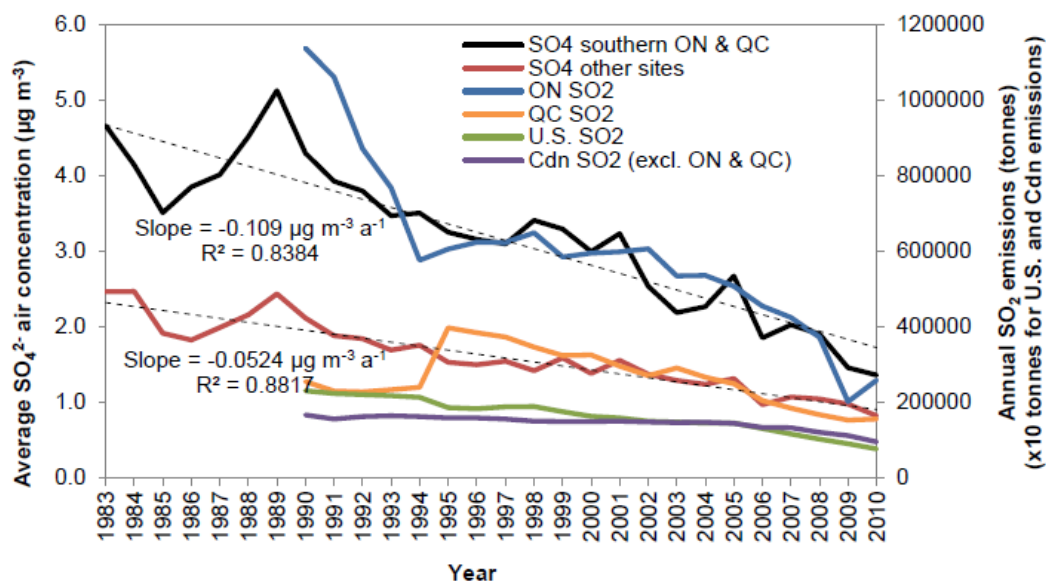


Figure 4: Temporal trends of annual average atmospheric SO_4^{2-} and annual SO_2 emissions. ON and QC refer to the province of Ontario and Quebec, respectively.

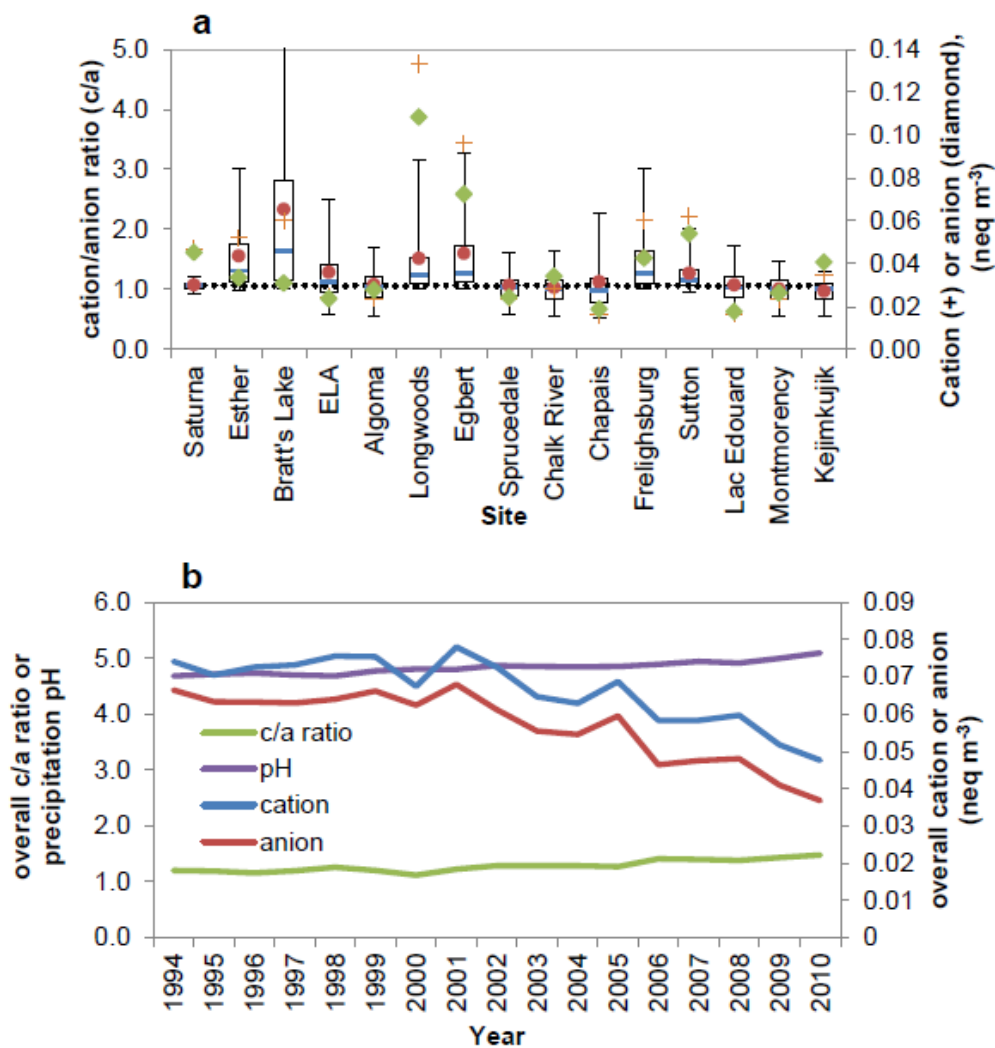
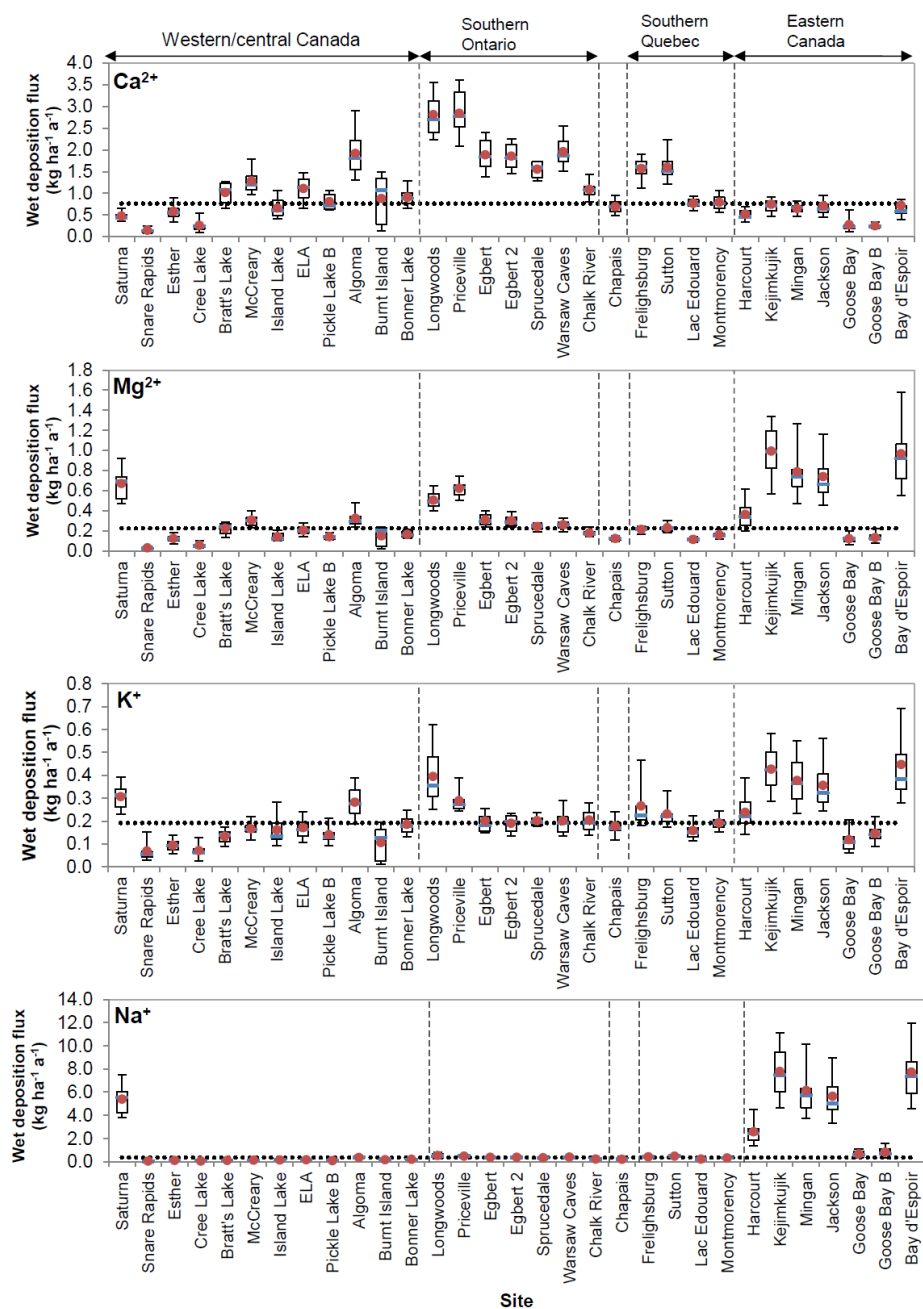


Figure 5: Geographical patterns of cation/anion (c/a) ratio and cation and anion concentrations (a) and temporal trends of annual average c/a ratio, cation and anion concentrations, and precipitation pH (b). In (a), the blue line indicates the median; the red dot indicates the mean; the box and whiskers include the interquartile range and the 5th to 95th percentile range, respectively; the dotted line is the overall median among the sites.



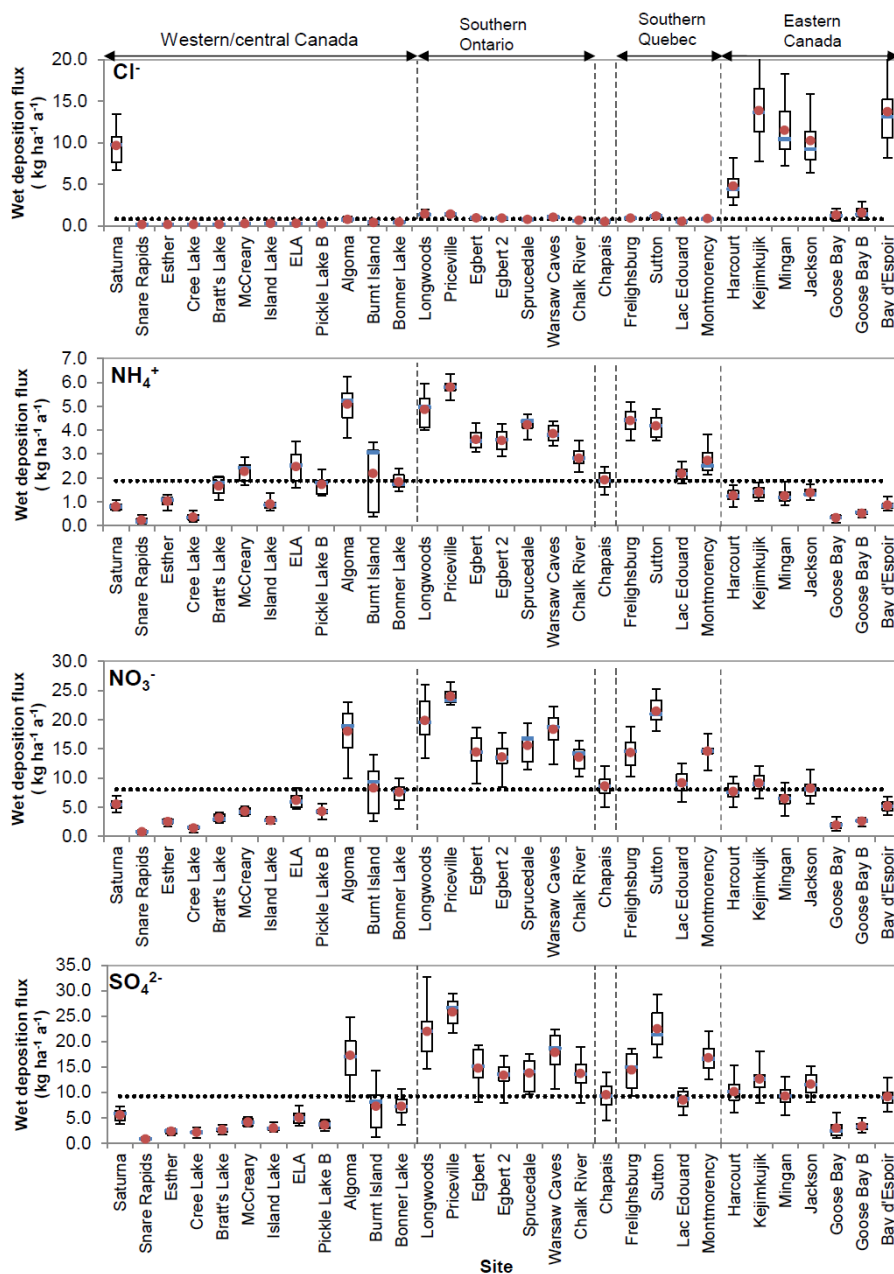


Figure 6: Geographical patterns of the annual wet deposition of ions. Sites are arranged in order from western to eastern Canada. The blue line indicates the median; the red dot indicates the mean; the box and whiskers include the interquartile range and the 5th to 95th percentile range, respectively; the dotted line is the overall median among the sites.

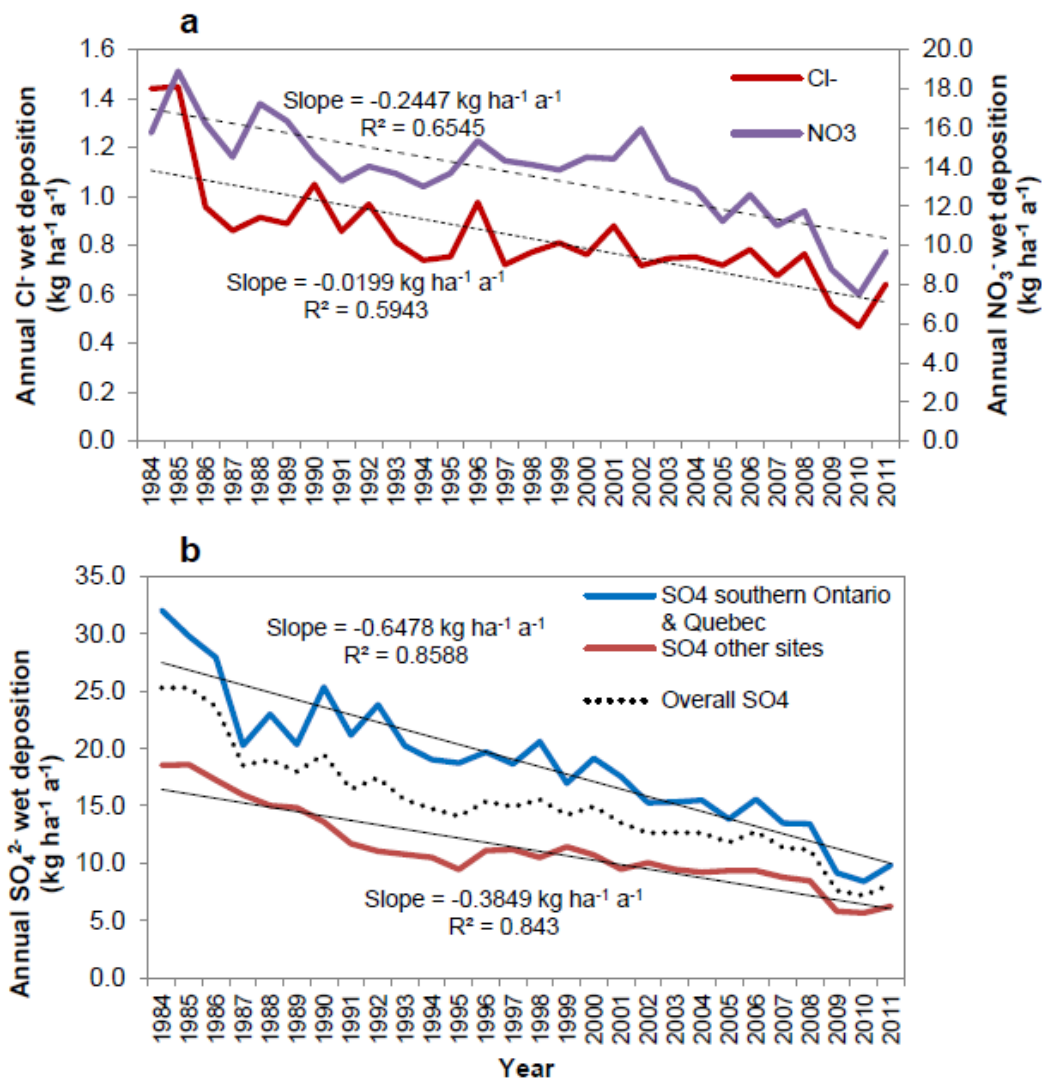


Figure 7: Temporal trends of annual wet deposition of Cl⁻ and NO₃⁻ (a) and SO₄²⁻ (b).

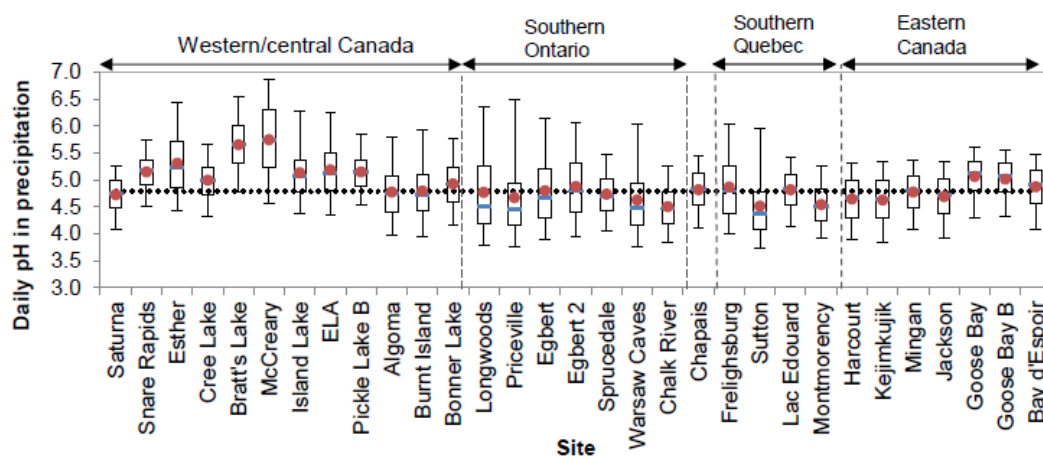


Figure 8: Geographical patterns of precipitation pH. See Fig. 6 caption.

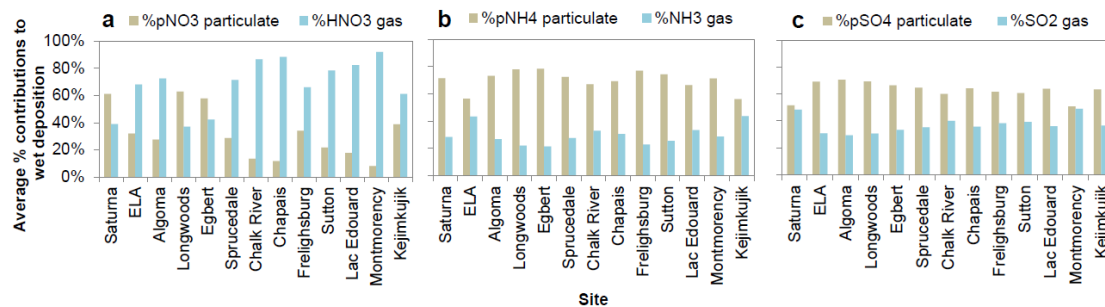


Figure 9: Average percent contributions of gas and particulate-phase species to nitrate (a), ammonium (b), and sulfate (c) wet deposition.

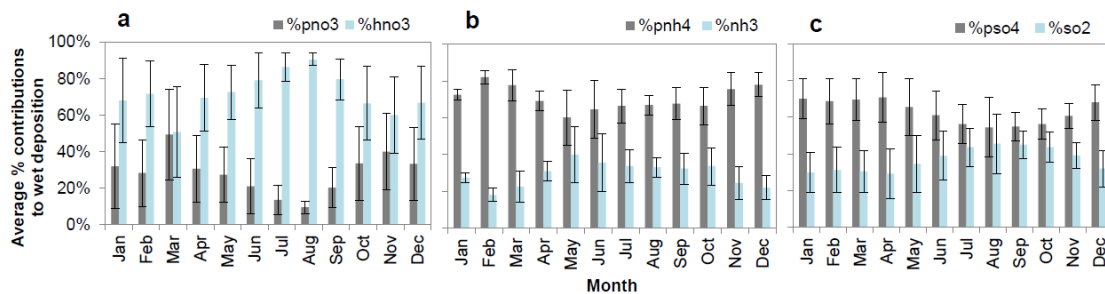


Figure 10: Monthly trend in the contributions of gas and particulate-phase species to nitrate (a), ammonium (b), and sulfate (c) wet deposition. Error bars represent the standard deviation of the percent contributions by gas and particulate-phase species between sites.